BIODEGRADABALE FLUORESCENT POLYMERS

by

SANTOSH GAUTAM

Presented to the Faculty of the Graduate School of

The University of Texas at Arlington in Partial Fulfillment

of the Requirements

for the Degree of

MASTER OF SCIENCE IN BIOMEDICAL ENGINEERING

THE UNIVERSITY OF TEXAS AT ARLINGTON

August 2008

ACKNOWLEDGEMENTS

I would like to express my deep and sincere gratitude to various people who made it easier for me to come up with this thesis. I would like to thank my father Sanu Babu Gautam for his loving support and continuous encouragement throughout my life. I would also like to thank my brothers Sushil and Saroj Gautam. Without their unconditional support and understanding, it would have been impossible for me to finish this project.

My utmost gratitude goes to my supervising professor, Dr. Jian Yang, for providing me this opportunity. Without his motivation, never-ending enthusiasm, continuous support and guidance, this work would remain unaccomplished. I would like to acknowledge Dr. Cheng-Jen Chuong and Dr. Wei Chen for accepting to be in my thesis committee. I sincerely appreciate them for providing their valuable time to go through the manuscript and offering me valuable advice. I would also like to thank my co-workers in the lab not only for their help but also for creating a friendly and interactive environment

Lastly, I am so grateful to my dear friends Binod, Jay and Purak for the support, energy and inspiration through this walk.

July 18, 2008

ABSTRACT

BIODEGRADABLE FLUORESCENT POLYMERS

Santosh Gautam, M.S.

The University of Texas at Arlington, 2008

Supervising Professor: Jian Yang

Most of the works done on fluorescent polymers are focused on their potential applications in lighting industries. Much less interest has been paid for their potential application in the field of biology and biomedical engineering. Although multiple biological uses of green fluorescent proteins (GFPs) have been addressed by different groups, their potential for biomedical applications is hampered by their tendency to photobleach rapidly and their short fluorescence lifetime. Quantum dots have emerged as a potential substitute for those applications, but their cytotoxicity and lack of biodegradability restrict their use in a biological system. An ideal fluorescent material that could be used for both biological and biomedical purposes should be biocompatible and biodegradable. They should have strong emissive property and high photostability.

The primary objective of this research was to develop biodegradable photolouminescent polymers (BPLPs) and nanoparticles using 1,8-Octanediol, Citric acid and different amino acids as the monomers. All of the twenty essential amino acids were used separately to create a family of BPLP. Owing to its better fluorescent properties, most of the experimental methods and discussion is based on BPLP with cysteine (BPLP-cys) in it. The

ratio between the monomers was also changed in order to fine tune the color and the mechanical properties of BPLPs. Different polymers and nanoparticles thus formed were characterized using fourier transformed infrared spectrometer (FTIR), nuclear magnetic resonance (NMR), ultra violet-visible spectrophotometer and fluorospectrophotometer. The tensile strength of BPLP-cys was found to be in a range of 3.2±0.13 to 6.5±0.8 MPa and its modulus was as high as 7.02±1.40 MPa. BPLP-cys had a maximum elongation up to 240±36 %. The results from transmission electron microscopy (TEM) indicated a size that ranged between 50 to 450 nm for various concentrations of BPLP-cys. The polymers were shown to be cytocompatible through various cell culture studies. Lastly, BPLPs incorporated with other amino acids emitted light in various regions of visible spectrum. Hence, the family of BPLP can prove to be helpful in multi-color imaging applications.

TABLE OF CONTENTS

LIST OF ILLUSTRATIONS

LIST OF TABLES

CHAPTER 1

INTRODUCTION

The materials containing either aromatic or heterocyclic units in them have a delocalized electron system [1-9]. The delocalized electron system is capable of absorbing light due to π-π^* transition. The absorbance of light energy will lead those units to a relatively unstable excited state. The excited units have a tendency to return to the ground state either radiatively or non-radiatively [1, 7]. The radiative way of returning to the ground results in an emission of light and the process is often referred to as 'fluorescence' [7]. The materials that have such a capability are fluorescent materials. The commonly known fluorescent materials a re synthetic polymers, organic dyes, green fluorescent proteins (GFPs) and quantum dots. In this chapter we will try to give an overview, synthesis, application and shortcoming of each type of fluorescent materials. The discussion will primarily be based on biological, biotechnological and tissue engineering aspects.

1.1 Synthetic Fluorescent Polymers

1.1.1 Brief Description

Synthetic polymers are human made organic materials that have been an integral part of everyday life. Their flexibility and versatility count for their importance in multiple areas such as industrial, biotechnological and medicinal. Recently, synthetic polymers with light emitting properties have been a part of relentless research because they are considered to be suitable for several applications in lighting industries. The ease of processability, low-operating voltages, easy color tuning, fast response time, and high quality of display are some of their advantages over conventionally used organic materials [1, 6].

Several small molecular units called monomers are added together using different polymerization techniques in order to synthesize polymers. The polymerization techniques can be classified as chain polymerization and step-growth polymerization [10]. Chain polymerization, also known as addition polymerization, involves the addition of monomers in one reactive end of a growing chain [11]. In contrast to a chain polymerization, a step-growth polymerization, also known as condensation polymerization, involves reaction with all monomer species [11]. Usually monomers present in such a polymerization contain reactive groups on both ends [11]. The commonly used monomers for the synthesis of fluorescent polymers include phenyl, vinyl and conventional unsaturated compounds or their derivatives [7].

1.1.2 Applications

The works on light emitting polymers has been gaining its ground for its multiple applications such as light emitting diodes (LEDs), field effect transistors (FET), photovoltaic cells, flat panel displays, etc. [1-3, 9] . Ever since Burroughes et al first showed the possible application of fluorescent polymers in the light emitting diodes in 1990, numerous such works has been reported [12, 13]. Apart from their light emitting properties, fluorescent polymers are advantageous for some electronic applications because of their processability and mechanical flexibility [2, 6].

1.1.3 Limitations

The structural and the mechanical properties of fluorescent polymers have been exploited by different groups in order to optimize their efficiency [1, 2, 14]. Some groups have focused on improving the intensity of fluorescence, whereas other are concentrated on the color tunability of those materials or both at once. However, among the three basic colors (red, green and blue), the quest for blue light emitting polymer with high efficiency and good color purity still has remained a challenge [4]. Efficiency and color purity of blue light emitting polymers have

been a major challenge to date [5]. Highly efficient blue light emitting diode is still sought [6]. Fluorescent polymers have not been used for tissue engineering purposes to our knowledge.

1.2 Organic Dyes

1.2.1 Brief Description

Fluorescent polymers have other applications apart from LED. They can be used as dyes. Dyes can be classified in two ways a) organic or inorganic, and b) natural or synthetic [15]. Organic dyes are the most commonly used dyes. They are capable of absorbing and emitting variable colors in visible range and hence are considered to be useful for multi-color imaging applications. Nitro, nitroso, azo, sulfur, and carbonyl dyes are most commonly used dyes and all of them contain a conjugated system [15].

1.2.2 Applications

The applications of fluorescent dyes depend on their chemical properties and binding specificity [16]. In the field of biology, fluorescent dyes serve three basic functions as: labels for biomolecules, cellular stains and enzyme-substrates [17]. The biological applications of fluorescence dye lie in but not limited to the areas like proteomics, gene technology, cell tracking, immunoassay, in vivo imaging and in vivo tracking of biochemical processes [16, 18, 19].

1.2.3 Limitations

Despite their multiple applications, organic dyes have limitations. Most of the organic dyes are not used for in vivo purposes because they exhibit poor photostability [20-22]. The organic fluorophores are found to bleach after only a few minutes of exposure to the light [18]. Another problem with organic dyes is their relatively short fluorescence lifetime. The fluorescence lifetime of less than 5 ns coincides with that of autofluorescence of cells and

tissues which means a reduction in a signal-to-noise ratio [18, 22]. Their difficult conjugation chemistry is another limitation of organic dyes.

1.3 Green Fluorescent Proteins

1.3.1 Brief Description

Green fluorescent protein (GFP) is another type of commonly used fluorescent material. GFPs are the proteins extracted from a jellyfish *Aequorea victoria* [23]. Although GFPs emit the best in the green region of a visible spectrum, the quest for optimizing GFPs for multiple color emission is still ongoing. The instances of development of blue fluorescent protein from the mutants of green fluorescent protein have also been reported too [24-26].

1.3.2 Applications

GFPs are largely used as a fluorescent labels mostly in the area of biochemistry and cell biology. They can be expressed in situ by gene transfer and their spontaneous fluorescent properties can be coupled for imaging applications [27]. Blue fluorescent proteins (BFP) are considered to be useful in lifetime imaging studies and also as Förster Resonance Energy Transfer (FRET) donors to GFP [26]. They are considered to be helpful to monitor the biological process at both small and large scales such as cell sorting, enzyme tracking and whole organism visualization. [28].

1.3.3 Limitations

Despite their potential to be used, the optimization in color tuning is still lacking. For example, the utility of BFPs is largely hampered by their low quantum yield [24]. Their emission is very dim both in vivo and in vitro due to low quantum yield [25]. Out of the reported BFPs, the mutant type P4 and P4-3 have a quantum yield of 0.21 and 0.38 respectively [25]. Different residues like F64L/V163A, Azurite, A5, etc have been incorporated into the parental BFP in

order to optimize the quantum yield and a maximum of 0.55 efficiency has been reported [26]. Increasing the quantum yield of blue fluorescent protein still remains a challenge to achieve a better resolution in imaging. Fluorescence lifetime is another shortcoming of green fluorescent proteins. They have a very short fluorescent lifetime ranging from picoseconds to a couple of nanoseconds [26]. They also suffer from photobleaching which reduces the chances in their detectability [29, 30].This hinders their potential application in lifetime imaging studies.

1.4 Quantum Dots

1.4.1 Brief Description

Inorganic nanoparticles called quantum dots have now emerged as an alternative fluorescent material to conventional fluorescent dyes. Quantum dots have a size of about 1-10 nm and are generally derived from a variety of semiconducting materials [31]. At this size, those particles partly retain the property of the material it is derived from and part of the properties will be newly acquired [32]. Quantum dots are best known for their ability to emit all the colors of a visible spectrum.

1.4.2 Applications

Because of their dimensional similarities with biological macromolecules, ability to emit different colors, better photostability and shorter lifetime, quantum dots have been preferred over the organic dyes and fluorescent proteins in most of the fluorescent-based applications [18, 20, 31-34]. Due to their ability to emit narrower emission spectra, they are considered for the experiments that need a purity of color.

1.4.3 Limitations

Despite all these features, quantum dots are biologically incompatible because they consist of a core of variety of metal complexes like cadmium and selenium [31, 35-37]. The

desorption of free metal ions from the core, free radical formation and their interaction with the intracellular contents are thought to be the reasons behind the cytotoxicity of nanoparticles [18]. The cytotoxicity of quantum dots both in vivo and in vitro have been reported by several groups [38-42]. Another disadvantage of quantum dot is its hydrophobic nature [43]. In order to make them hydrophilic, quantum dots core are often coated with the cell friendly materials [21]. Coating the hydrophobic core with hydrophilic compounds reduces the cytotoxicity of quantum dots, but there still exists a concern for their long term effect in a body due to lack of biodegradability of the core [21].

1.5 Tissue Engineering

Tissue engineering is an upcoming interdisciplinary field that applies the principles of engineering and life sciences toward the development of biological substitutes that restore, maintain, or improve tissue function [44]. Various properties of cells are exploited in order to develop such an ideal substitute required to regenerate tissues.

1.5.1 Biomaterial and Scaffold

Cells are found to be growing in the extracellular matrix (ECM) found in the body. Scaffold serves the purpose of ECM and provides the platform for the cellular growth. Scaffold is a porous structure made out of a biomaterial in a variety of shapes and sizes. The proper size and porosity play an important role in cellular infiltration and vascularization [45]. Scaffolds are often incorporated with growth and differentiation factors so that cells could be guided with physical and chemical cues to differentiate and assemble into three dimensional tissues [46]. It is desirable that the biomaterials used for tissue engineering purpose are easily process able, biodegradable and biocompatible.

1.5.2 Biodegradability

Biodegradation is defined as the chemical breakdown of materials by the action of living organisms [47]. Controlled biodegradability is considered to be a useful parameter while designing the biological constructs. Biodegradable nature of scaffold facilitates the formation of new tissues and reduces the long term worries regarding the implanted materials [45].

1.5.3 Biocompatibility

Biocompatibility is an important factor to be considered while designing the biological constructs. It is defined as an ability of material to perform with an appropriate host response in a specific application [47]. A biologically incompatible material might be a target of body's host response system and might not serve the function too well.

The basic idea of tissue engineering is to regenerate tissues by isolating and seeding cells into the biodegradable scaffolds. Scaffolds are often provided with growth and differentiation cues. The cell seeded scaffolds are then implanted into the desired site for further regeneration process in natural environment. The cells start to synthesize its own extracellular matrix and scaffold will slowly degrade facilitating the regeneration of new tissue.

1.6 Overview of Research Project

In reviewing the trends of utility of different fluorescent materials, it is found that the existing materials and techniques suffer in one way or the other when it comes to applications. The organic dyes suffer from broad spectral overlap, photobleaching, short fluorescence lifetime, difficult conjugation chemistry and even cytotoxicity in some cases. The fluorescent proteins suffer from photobleaching, shorter fluorescence lifetime and low quantum yield.

Similarly, quantum dots raise the question of cytotoxicity, interference with physiological activity and the long term effects are yet to be analyzed. Different modifications that are needed

to conjugate the quantum dots with the biological units are another disadvantage of quantum dots.

An ideal fluorescent material that is used for in vivo imaging should be biocompatible and biodegradable. They should readily undergo bioconjugation so that the cellular/molecular detection will be easier. They should also be photobleaching resistant. Higher quantum yield is desirable.

1.6.1 Goals and Objectives

The primary purpose of this project was to generate a novel class of fluorescent polymer that can prove to be useful for multiple applications in biology and biomedical engineering. For organic dyes like purpose, polymer that is dissolvable in both organic solvents and water were developed. In order to develop the possibility of controlled and targeted drug delivery system, citric acid, a compound found in biological system, was used as a monomer. With a carboxyl group in its backbone, those polymers can serve the purpose of bioconjugation for drug delivery system. They carry a potential to be conjugated with different biological molecules and can be used for imaging applications. Unlike other organic fluorophores used so far, their potential of nanoparticles generation should make these polymers preferable over the others. Biodegradability and biocompatibility of polymers and their nanoparticles are important properties in order to ensure their potential use in humans. The generation of fluorescent nanoparticles was aimed at their potential to be used in DNA hybridization assays, immunodetection assays, biosensing, labeling macromolecules and in vivo/in vitro imaging. They have a potential application in the field of drug delivery. Good mechanical properties and biocompatibility were desired properties from scaffolds and films for tissue engineering applications. The goal of making fluorescent scaffold was to analyze the possibility of monitoring the scaffold degradation and tissue regeneration on scaffold in situ without undergoing animal-sacrificing and tedious histological procedures. As a blue light emitting polymer, its potential

application in the manufacturing of light emitting devices was equally considered. Overall, the development of BPLPs aimed to represent a paradigm shift of photoluminescent materials and to have a wide impact on the many fields including biomedical and non-biomedical fields.

1.6.2 Specific Aims

- Aim 1: Synthesize photoluminescent polymers and nanoparticles.
- Aim 2: Characterize their fluorescent properties, chemical composition, mechanical, biodegradable and biocompatible properties.

1.6.3 Innovative Aspects

There are several novel aspects involved in the development of those polymers. This is, for the first time to create a family of biodegradable photoluminescent polymers, BPLPs. Synthetic fluorescent polymers are commonly made out of either heterocyclic or aromatic units and their copolymers. BPLPs are novel synthetic fluorescent polymers synthesized using simple monomers without conjugated system. Another novel aspect of this research is the fluorescent degradable nanoparticles and scaffold for tissue engineering. Commonly, the synthetic fluorescent polymers emit one specific color. The capability of BPLPs to emit light in wide spectrum of color is another innovative aspect.

CHAPTER 2

EXPERIMENTAL

2.1 Materials

All the chemicals required for this project were purchased from Sigma and were used without further purification.

2.2 Methods

2.2.1 BPLP Synthesis

Water soluble and organic solvent soluble polymers were synthesized using the monomers mentioned above.

2.2.1.1 BPLP Synthesis Using Cysteine

Equimolar amounts of citric acid and 1,8-Octanediol were added to a 250-ml three necked round bottom flask fitted with the electromagnetic stirrer, an inlet adapter and an outlet adapter. For each mole of citric acid and 1, 8-Octanediol, 0.2, 0.4, 0.6 and 0.8 molar of cysteine was added to the round bottom flask to continue four different sets of reaction. The mixture was melted at 165^0C under a flow of nitrogen gas while stirring. The temperature of the system was brought down to 140^0C after the monomers melted down. The reaction was proceeded for another 75 minutes under stirring to get the pre-polymer. The pre-polymer was dissolved in 1,4-Dioxane and was precipitated in water followed by freeze drying.

2.2.1.2 Water Soluble BPLP Synthesis

The water soluble fluorescent polymer was synthesized by taking equimolar amount of poly (ethylene glycol) (PEG) and citric acid followed by the addition of cysteine later. A similar

method explained earlier was used for the synthesis except for the precipitation part. The water solubility of this polymer forbids precipitation method to purify the polymer. Thus, the polymer was purified using the dialysis method followed by freeze drying. The polymer was named BPLP-PEG-cys.

2.2.1.3 Synthesis of BPLPs with Rest of the Amino Acids

The rest of the nineteen amino acids found in biological systems were used to synthesize the fluorescent polymer with citric acid and 1,8-octanediol using the above protocol.

The polymers are denoted as BPLP-amino acid. For example, when serine was used, it was referred to as BPLP-serine or BPLP-ser.

2.2.2 Preparation of Polymer Films

The films can be made by postpolymerizing the pre-polymers at high temperature. BPLP-cys was dissolved in 1, 4-dioxane to form a 30 wt % solution. The resulting mixture was cast into a Teflon mold of desired diameter. After solvent evaporation for 24 h, the mold was transferred to the 80 ^{0}C oven. The polymeric film was taken out after four days of postpolymerization. The postpolymerized (crosslinked) polymers were denoted as CBPLP-amino acid. For example, when cysteine was used, its crosslinked form was denoted as CBPLP-cysteine or CBPLP-cys.

2.2.3 Scaffold Fabrication

The scaffold fabrication was done using a common salt leaching method. A 30 % solution by weight of polymer was made in 1,4-Dioxane. The polymer solution was added with sieved salt crystals which served as a porogen. This salt/pre-polymer slurry was cast into a square Teflon mold which was then transferred into the 80^{0} C oven. After 4 days of post-polymerization, the salt in the resulting composite was leached out by successive incubations in

deionized water (produced by a Millipore water purification system, Millipore, Billerica, MA, USA) every 12 h for 96hr. The porous scaffold was then freeze-dried for 24 h to get rid of the water contents.

2.2.4 Preparation of Nanoparticles

The nanoparticles were prepared using a nanoprecipitation technique [48]. 10 mg of a polymer was dissolved in 10 ml of acetone. The polymeric solution was added dropwise to 100 ml of deionized water under magnetic stirring at a speed of about 400 rpm. The setup was left overnight in a chemical hood to let the acetone evaporate.

2.3 Measurement and Characterization

2.3.1 FTIR

The pre-polymer was dissolved in 1, 4-Dioxane to make 5 % solution by weight. It was casted over a KBr pellet. The solvent was let evaporate overnight in a chemical hood. Fourier Transform Infra Red (FTIR) spectra were collected at room temperature using Nicolet 6700 FTIR spectrometer (Thermo Fisher Scientific). The spectrum was taken from 4000 cm^{-1} to 400 $cm^{-1.}$

2.3.2 ^{1}H- NMR and ^{13}C- NMR

5 mg of polymer was dissolved in 1 ml of deuterated dimethyl sulfoxide (DMSO). The ^{1}H-NMR was recorded at room temperature on JEOL 300 Hz spectrometer, whereas the ^{13}C-NMR was recorded on JEOL 500 Hz spectrometer. Tetramethylsilane was used as reference in both cases.

2.3.3 Ultra Violet-Visible Spectroscopy

A dilute solution of pre-polymer (less than 1 % w/w) was prepared in 1, 4-Dioxane. The path length of a quartz cuvette was 1 mm. The scan speed was set to medium and the sampling interval was 0.5 nm. Ultraviolet-visible absorption spectra were collected using a SHIMADZU UV-2450 spectrophotometer.

2.3.4 Photoluminescence Spectra

All photoluminescence spectra were obtained using SHIMADZU RF-5301 PC fluorospectrophotometer. The sample (5% w/w) in a quartz cuvette of 10 mm path length was excited at 350 nm. The optimal emission wavelength was determined first from the excitation spectra. The emission spectra were then collected using the optimal excitation wavelength. Both the excitation and the emission slit width were set at 1.5 nm for all samples unless otherwise stated.

2.3.5 Photoluminescence Quantum Yield

In order to measure the fluorescent quantum efficiency of the polymer, the well-known Williams' method was used [49]. In this comparative method, well characterized dyes such as rhodamine, coumarin, anthracene, etc of known quantum efficiency are used as standards. In this case, anthracene (quantum yield = 0.27 in ethanol) was used as a standard. The polymer and anthracene both were dissolved in ethanol. Concentration of both the sample and the standard were adjusted so that their absorbance was always lesser than 0.1. The absorbance of less than 0.1 is desirable in order to avoid the reabsorption effect. Absorbances of both were measured using a SHIMADZU UV-2450 spectrophotometer. Their absorbance at 350 nm was noted. Then, they were excited at 350 nm using SHIMADZU RF-5301 PC fluorospectrophotometer. Multiple concentrations of both the standard and the sample were prepared and the same steps were repeated to obtain their absorbance and intensity. Intensity

obtained was plotted against the corresponding absorbance to get a curve which is linearized to get a gradient for both the sample and the standard. The absolute quantum efficiency for a given sample was calculated using the following equation:

$$\Phi_X = \Phi_{ST}\left(\frac{Slope_X}{Slope_{ST}}\right)\left(\frac{\eta_X}{\eta_{ST}}\right)^2 \quad (1)$$

where,

Φ_X = Quantum efficiency of the sample

$Slope_X$ = Slope of the curve obtained from the intensity versus absorbance plot for the sample

η_X= Refractive index of the solvent used to dissolve the sample

Φ_{ST} = Quantum efficiency of the standard

$Slope_{ST}$ = Slope of the curve obtained from the intensity versus absorbance plot for the standard

η_{ST}= Refractive index of the solvent used to dissolve the standard

2.3.6 Mechanical Characterization

The tensile mechanical tests were conducted according to ASTM D412a on a MTS Insight 2 mechanical tester equipped with 500N load cell. 4-6 specimens of each polymeric ratio were cut into dog bone shape (26 x 4 x 1.5 mm). The samples were clamped and pulled at a rate of 500 mm/min. The Young's modulus was measured from an initial slope and the average for each ratio was calculated. The crosslinking density (n) was calculated using the following equation derived from the theory of rubber elasticity equation [50, 51].

$$n = \frac{E_0}{3RT} = \frac{\rho}{M_c} \quad (2)$$

where,

E_0 = Modulus of elasticity

R= Universal gas constant

T= Absolute temperature

ρ = Polymer density at a given temperature

M_c = Molecular weight between crosslinks

2.3.7 In Vitro Degradation Study

The preliminary study of degradability of polymers was done in vitro. Pre-polymers with two different molar ratios of cysteine were chosen. About 50 mg of pre-polymer was placed in a tube containing 10 ml of phosphate buffer saline (pH=7.4). All the samples were incubated at 37 ^{0}C for predetermined time points. The samples were taken out and washed with water at those time points. They were freeze dried for a week. The mass loss was calculated using the following equation

$$\text{mass loss } (\%) = \frac{w_0 - w_t}{w_0} \times 100 \qquad (3)$$

where,

w_0 = initial weight of pre-polymer, and

w_t = weight of pre-polymer at a given time point

2.3.7.1 Photoluminescence Spectra of Degraded Samples

In order to analyze the effect of degradation of polymer on their fluorescent properties, the degraded samples at different time points were taken. The samples were dissolved in 1,4 - Dioxane to make a 5% polymer solution by weight. The photoluminescence spectra were

collected by SHIMADZU RF-5301PC fluorospectrophotometer using the protocol mentioned above.

2.3.8 Cell Culture Study

For the purpose of a cell culture study, BPLP-cys films were cut into pieces (diameter 7mm). The film was incubated in ethanol for 30 min and then exposed to UV light for another 30 min in order to sterilize it. The cells were cultured in 75 cm^2 tissue culture flasks with Dulbecco's modified eagle's medium (DMEM), which had been supplemented with 10% fetal bovine serum (FBS). Culture flasks were kept in an incubator maintained at 37 °C, 5% CO_2 and 95% humidity. The cells were trypsinized, centrifuged and suspended in media to obtain a seeding density of $3x10^5$ cell/ml for the films. A seeding density of $8x10^5$ cell/ml was used for seeding on the scaffolds. 200 µl of the cell suspension was distributed on top of the polymer specimens in the culture dishes. After 1 hour of incubation at 37 °C, 5 ml of media was added to each culture dish. Cell growth and proliferation was allowed on the films and scaffolds for 3 days and 7 days respectively. The confluent cells were fixed by addition of 2.5% gluteraldehyde solution followed by incubation of 2h. The samples were then dehydrated in 50%, 75%, 95% and 100% ethanol sequentially. This was followed by freeze drying. The samples were then sputter coated with silver and examined under the scanning electron microscope (SEM, Hitachi 3500N).

2.3.8.1 H & E staining

In addition to SEM observation, cell seeded scaffolds were also stained using hematoxylin and eosin stains. Briefly, cell seeded scaffolds were fixed with gluteraldehyde and sequentially dehydrated as per the aforementioned protocol. The fixed scaffolds were embedded in paraffin wax. 10µm sections were obtained from the scaffold embedded wax block using a HM310 microtome (Microm International., Walldorf, Germany). The sections were dewaxed, stained with hematoxylin and eosin and observed under a microscope.

2.3.9 Lifetime measurement

The output of a femtosecond regeneratively amplified Titanium: sapphire laser system operating at 1 kHz was used in order to collect the lifetime of the polymers. The 150 fs pulses of this laser at 400 nm were directed onto the polymer. Then, the emission was collected at right angles and focused into a streak camera (Hamamatsu C5680). Suitable bandpass and cutoff filters were used to collect the luminescence at different wavelengths. The time resolution of instrument was 200 ps full width at half maximum (FWHM). It was determined by using a standard scattering material.

2.3.10 Particle Size and Distribution

2.3.10.1 Transmission Electron Microscopy

In order to determine the size, shape and distribution of nanoparticles, the samples were prepared by drop casting nanoparticles (in water) onto a carbon coated copper grid. The samples were dried at room temperature. They were stained with Uranyl Acetate (UA) and were observed under TEM (JEOL-1200 EX II).

2.3.10.2 Size and Distribution of Nanoparticles

Dynamic light scattering (DLS) technology (Nanotrac. 150, Microtrac. Inc.) was used in order to determine the size and distribution of nanoparticles. The nanoparticles were prepared in de-ionized water and the measurement was done at room temperature.

CHAPTER 3

RESULTS

3.1 Characterization of BPLP-cys

3.1.1 IR Characterization

A typical FT-IR spectrum of pre-polymer is shown in figure 3.1. The presence of thiol (S-H) group is represented by a weak peak at 2575 cm^{-1} [52]. The peak at 1527 cm^{-1} corresponded to N-H deformation and C-N stretching of amide [53]. An intense peak at 1731 cm^{-1} represented the C=O stretch whereas the peak at 2931cm^{-1} was assigned to methylene groups [54]. The broad band at 3467 cm^{-1} was assigned to the hydroxyl group stretching vibration [55].

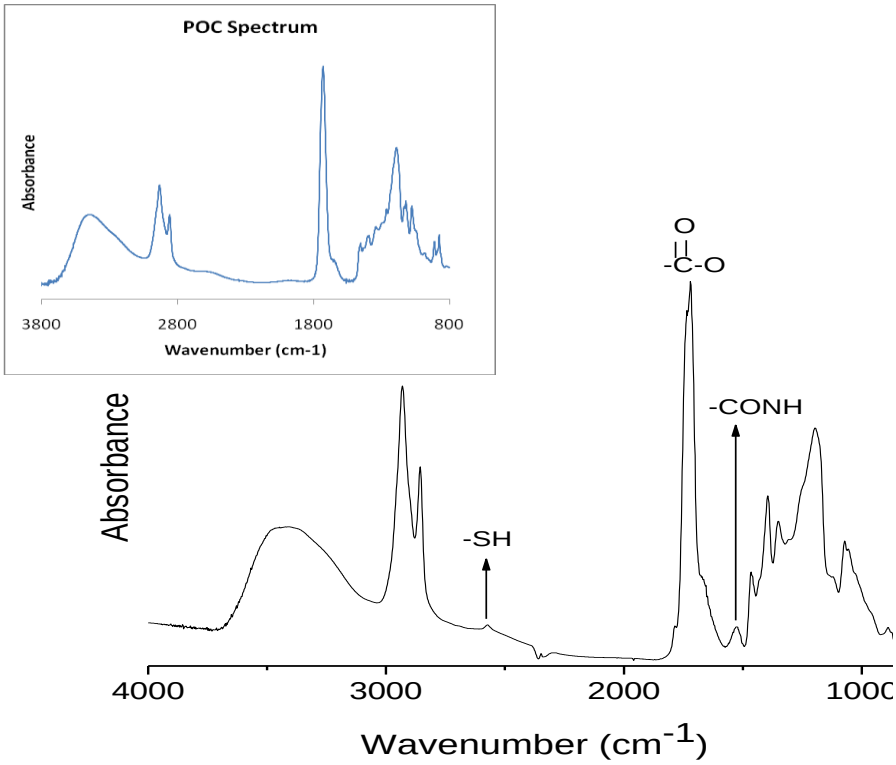

Fig 3.1: FTIR spectrum of BPLP-cys along with FTIR spectrum of poly(octanediol citrate) (inset).

3.1.2 ^{1}H-NMR and ^{13}C-NMR

Figure 3.2 represents the ^{1}H-NMR spectrum for BPLP-cys solution. The peak at 1.02 was assigned to –CH_2S**H** proton.

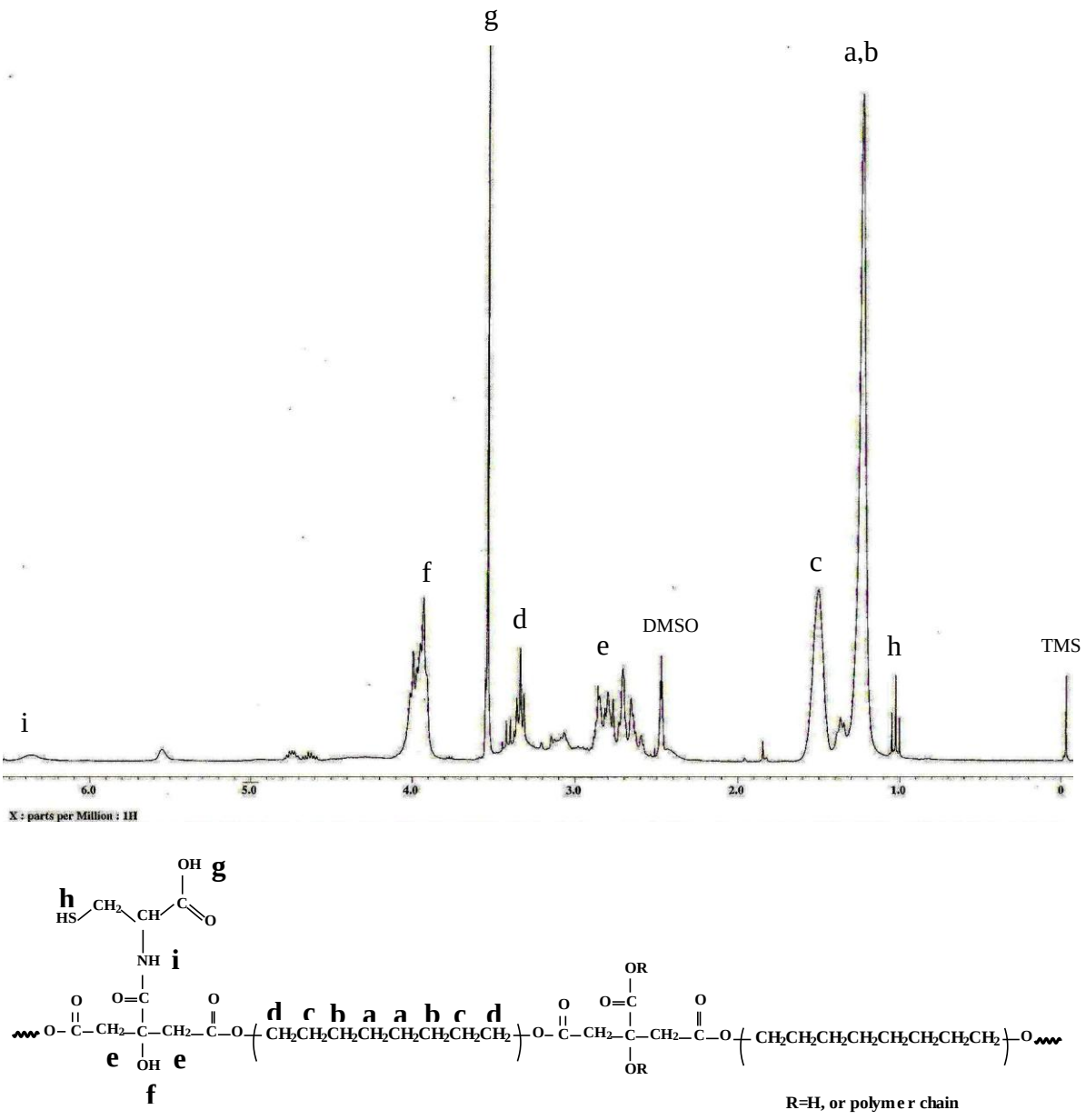

Fig 3.2: ^{1}H-NMR of BPLP-cys solution prepared in deutarated DMSO.

The peaks at 1.23 ppm and 1.50 ppm were assigned to the protons of –C**H$_2$**- from octanediol [54]. The multiple peaks at 2.75 ppm were assigned to protons of –C**H$_2$**- from citric acid [54].

The H-NMR spectrum for poly (Octanediol Citrate) (POC) is represented in figure 3.3 [54]. It was used for comparison with BPLP-cys H-NMR spectrum.

Figure 3.4 represents the ^{13}C-NMR of BPLP-cys. The peaks around 170 ppm were assigned to carbonyl (C=O) groups from citric acid and cysteine, whereas the peaks in between 20-30 ppm were assigned to –**C**H$_2$-carbons from octanediol [56]. The –O=C-**C**H$_2$- carbon was assigned at 61.2 ppm. The HN-**C**H- carbon of cysteine was assigned to the peak at 66.5 ppm [56]. The peak for central carbon atom of citric acid attached to hydroxyl group was assigned at 72.3 ppm.

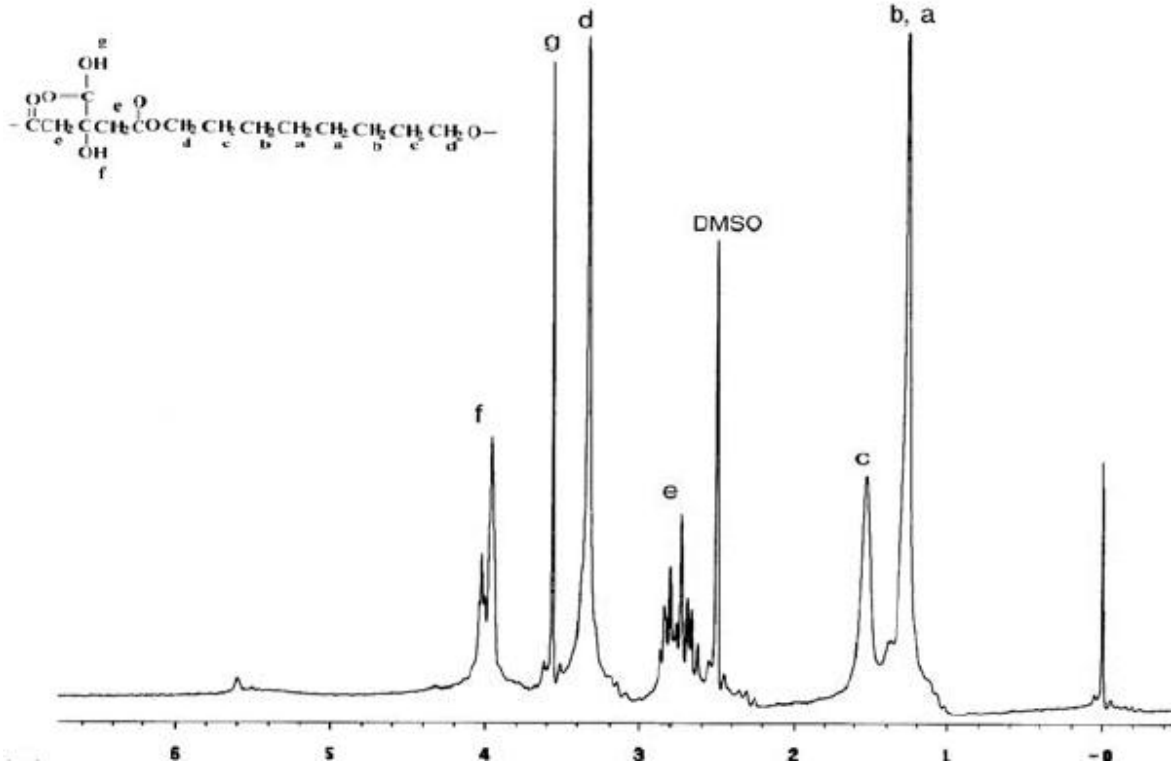

Fig 3.3 ^{1}H-NMR spectrum of Poly (Octanediol Citrate) (POC). POC does not have cysteine in it and was used as a control. The spectrum was taken from Yang et al [54] with author's permission.

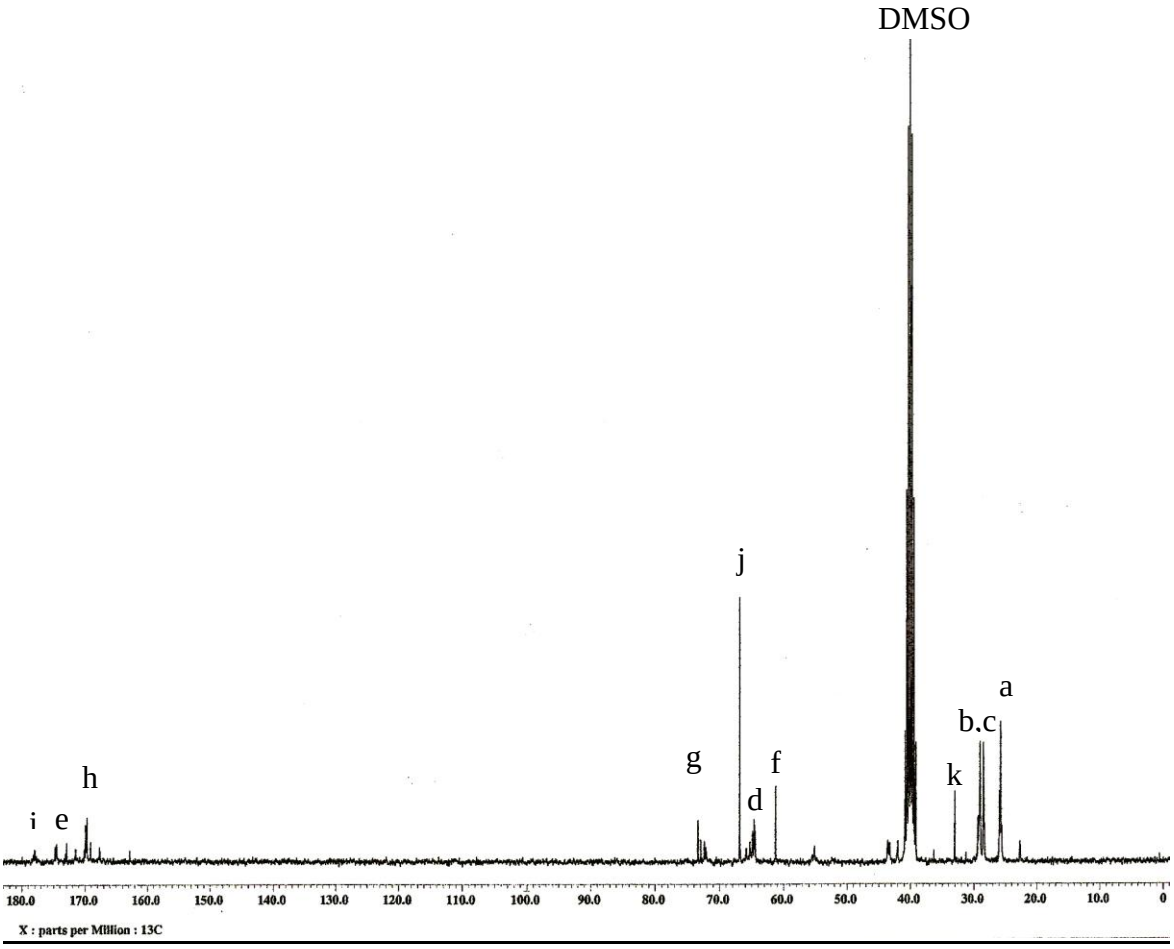

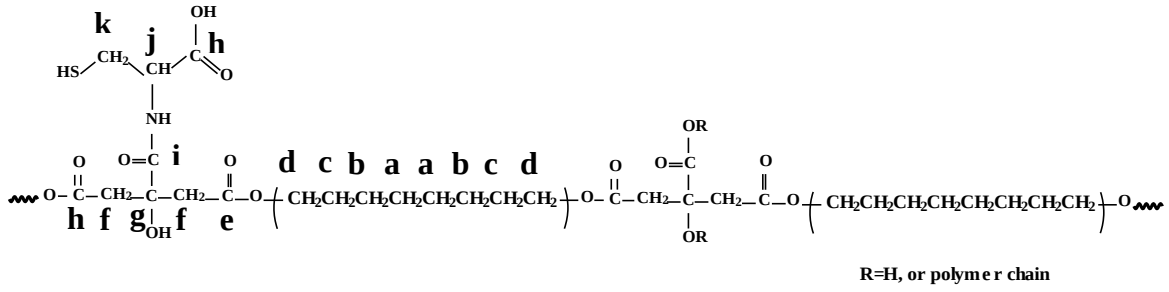

Fig 3.4: ^{13}C-NMR of BPLP-cys solution prepared in deutarated DMSO.

Based on FTIR and NMR results, we have proposed a synthesis route of BPLP-cys as shown in figure 3.5. The amine group of cysteine reacted with the –COOH group in a side chain of citric acid forming an amide bond.

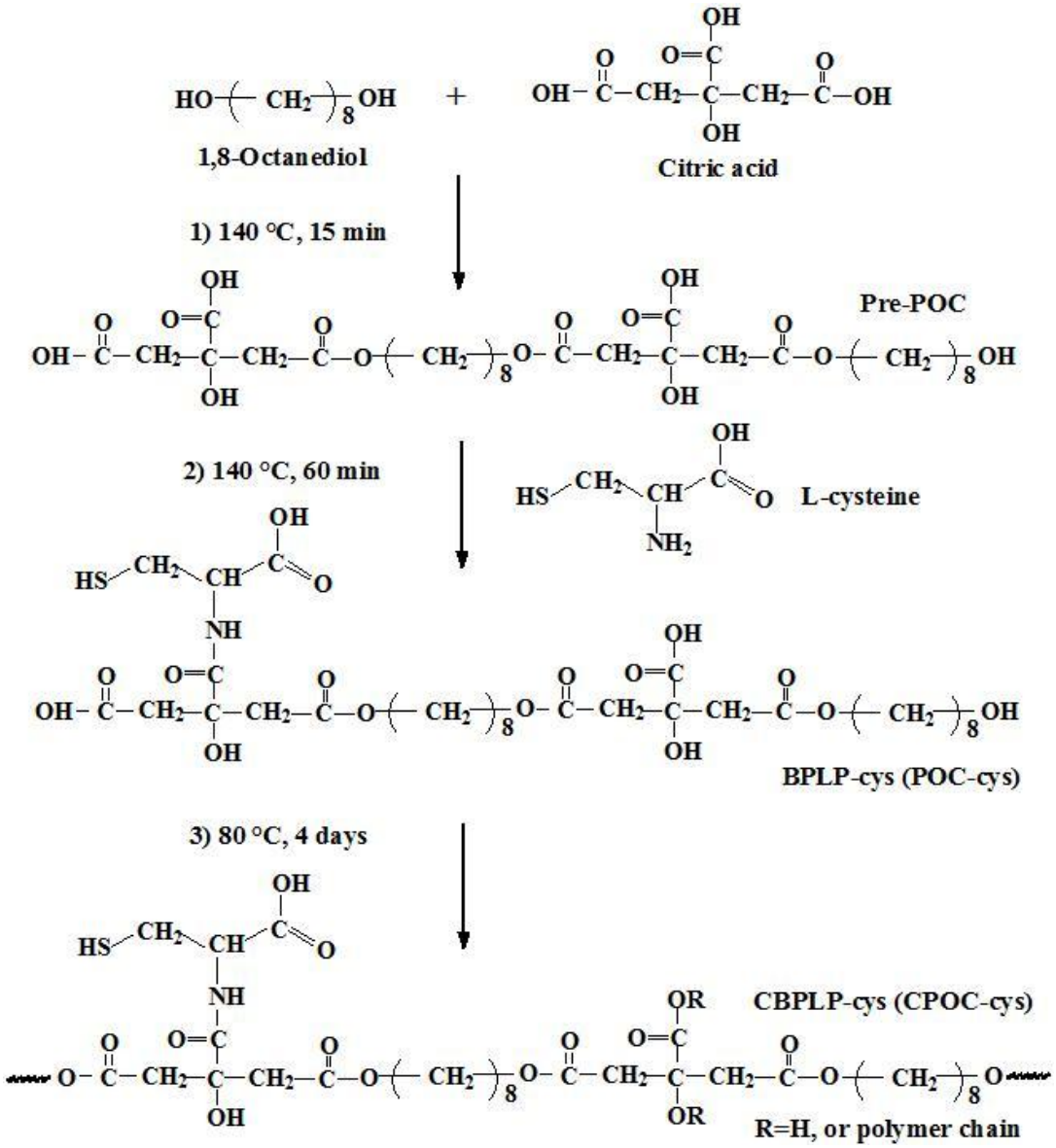

Fig 3.5: Proposed synthesis route of BPLP-cys and CBPLP-cys.

3.1.3 UV-vis Spectroscopy

The UV-visible absorption spectra for BPLP-cys with four different ratios of cysteine are shown in figure 3.6. BPLP-cys showed a single broad absorbance band with an absorbance maximum at 363 nm for all ratios. With an increasing amount of cysteine, the absorbance of BPLP-cys was found to be decreasing.

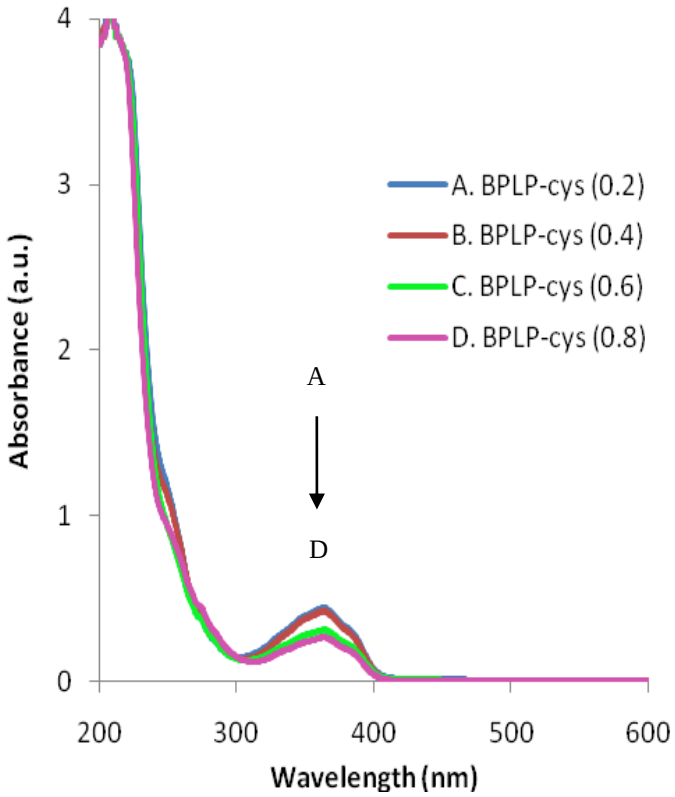

Fig 3.6: UV-vis spectra for BPLP-cys with different molar concentration of cysteine. A, B, C and D represent 0.2, 0.4, 0.6 and 0.8 molar concentration of cysteine present in polymer dissolved in dioxane.

3.1.4.Photoluminescent Spectroscopy

3.1.4.1 PL Spectra of BPLP-cys and CBPLP-cys

From the photoluminescent (PL) spectra of BPLP-cys, it was found that an excitation wavelength around 400 nm gave the optimum emission. At this particular wavelength, complete spectra for all the ratios couldn't be measured because of their high intensity that goes beyond the threshold of the fluorospectrophotometer. So, the PL spectra of BPLP-cys were measured with an excitation wavelength of 350 nm. The maximum emission for all ratios of BPLP-cys was observed at 435 nm, near the blue region of a visible spectrum as shown in figure 3.7. The photograph of BPLP-cys under different lighting conditions along with a control is represented in figure 3.15.

The PL spectrum of polymeric films (CBPLP-cys) is shown in figure 3.8. CBPLP-cys emitted blue light with an emission maximum at 439 nm. The fluorescence intensity of the films was found to be decreasing with an increasing amount of cysteine in the polymer. A slight red shift was also observed with increased ratio of cysteine. The photograph of CBPLP-cys under different lighting conditions along with a control film is represented in figure 3.16.

3.1.4.2 Excitation Spectra of BPLP-cys

A representative excitation spectrum of BPLP-cys is depicted in figure 3.9. The excitation spectrum of BPLP-cys consisted of two excitation maxima. The first one that appears at 328 nm was comparatively weaker. The second peak that was observed around 400 nm was intense. The excitation spectrum given in figure 3.9 was collected from 5% BPLP-cys 0.6 solution. At similar concentration, both the excitation (2^{nd} peak) and emission maxima of BPLP-cys 0.2 and 0.4 exceeded the threshold of the fluorospectrometer at a minimum possible slit width setting.

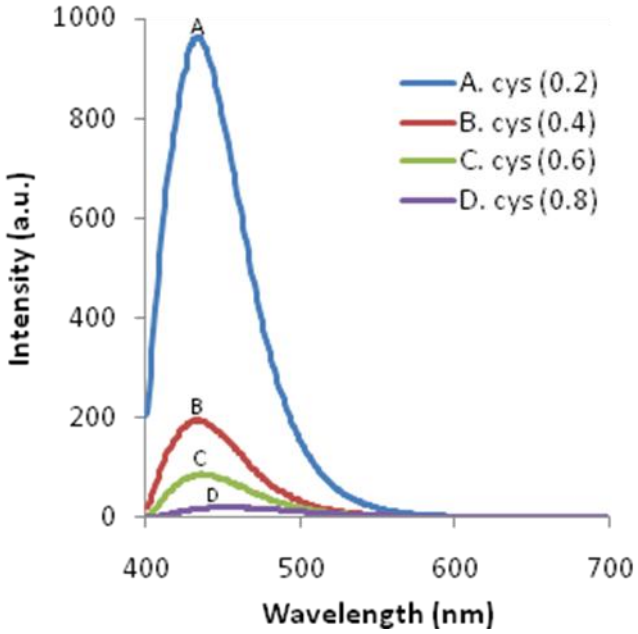

Fig 3.7: Emission spectra of BPLP-cys solution prepared in dioxane.

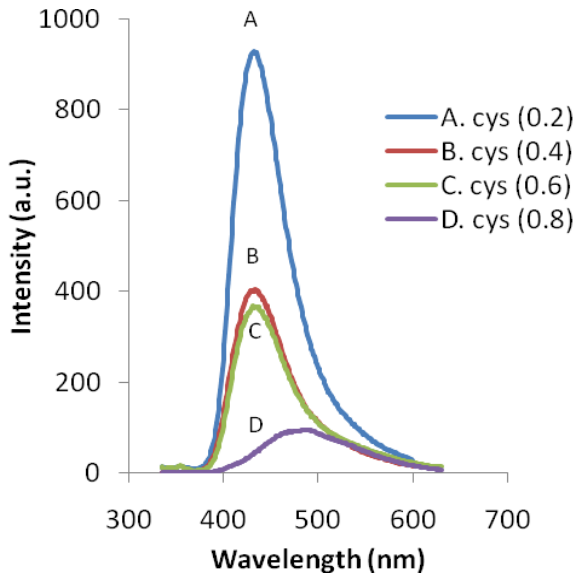

Fig 3.8: Emission spectra of CBPLP-cys polymer postpolymerized in 80^0 C oven for 4 days.

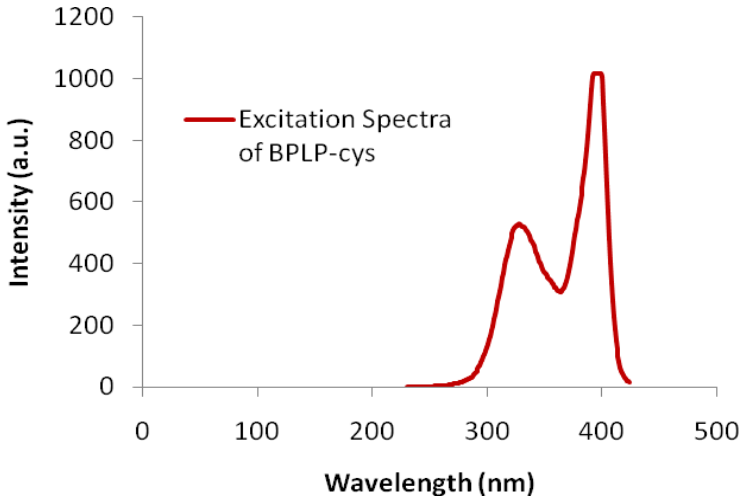

Fig 3.9: Representative excitation spectra of BPLP-cys showing multiple excitation maxima.

To ensure that the polymer acquired a novel fluorescent characteristics, that is not found in any of the monomers, the photoluminiescent spectra for monomers were collected. The results are depicted in figure 3.10.

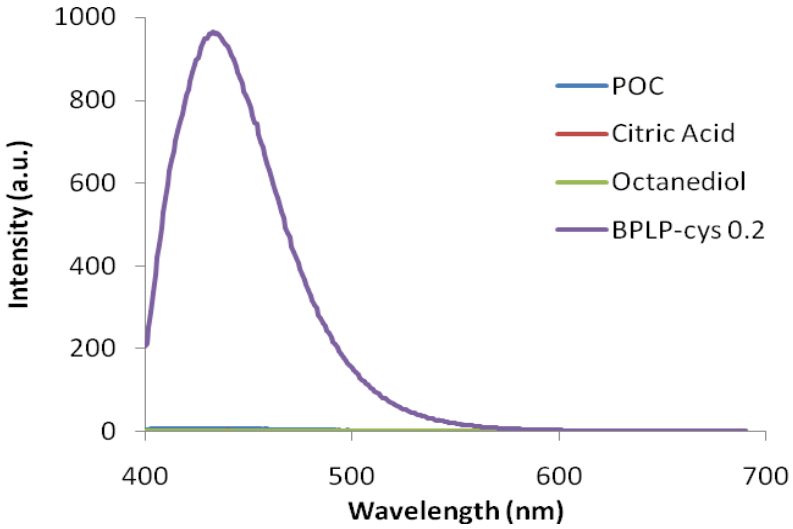

Fig 3.10 : Emission spectra of monomers used for synthesis along with BPLP-cys.

To have a better understanding of fluorescence mechanism, citric acid was replaced with succinic acid while synthesizing the polymer. Succinic acid does not have –COOH and –OH groups on its side chain like citric acid. The intensity of emission of such a polymer is much less than that of BPLP-cys (figure 3.11) .

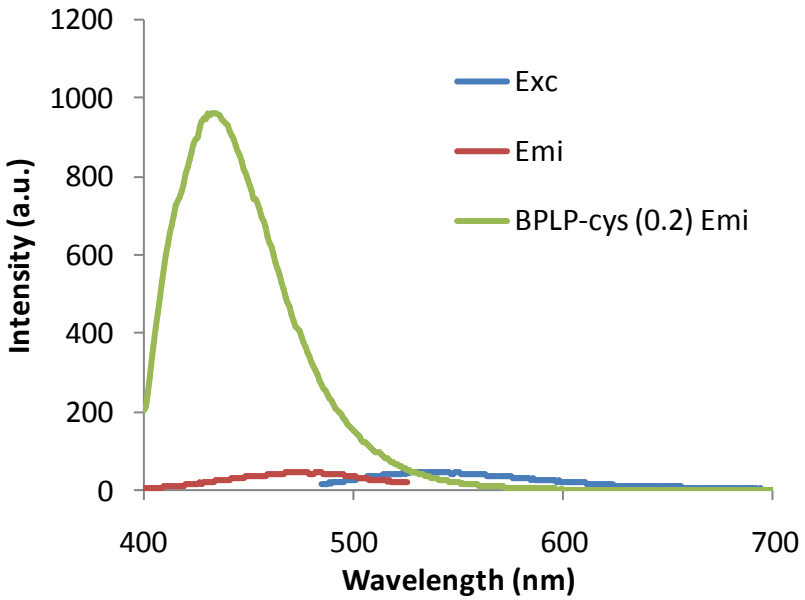

Fig 3.11: Photoluminescence spectra of succinic acid along with emission spectrum of BPLP-cys (0.2).

3.1.4.3 PL Spectra of BPLP-cys Scaffolds and Nanoparticles

The PL spectra for BPLP-cys scaffold and BPLP-cys nanoparticles are depicted in figure 3.12 and 3.13 respectively. The scaffold was excited at 380 nm to get an optimum emission with an emission maximum at 436 nm. Similarly, the nanoparticles in water were excited at 365 nm. The emission maximum for nanoparticles was found to be located at 433

nm. Scaffold had the least fluorescence intensity among films, solutions and nanoparticles. But, it was still bright enough as could be seen in Figure 3.17.

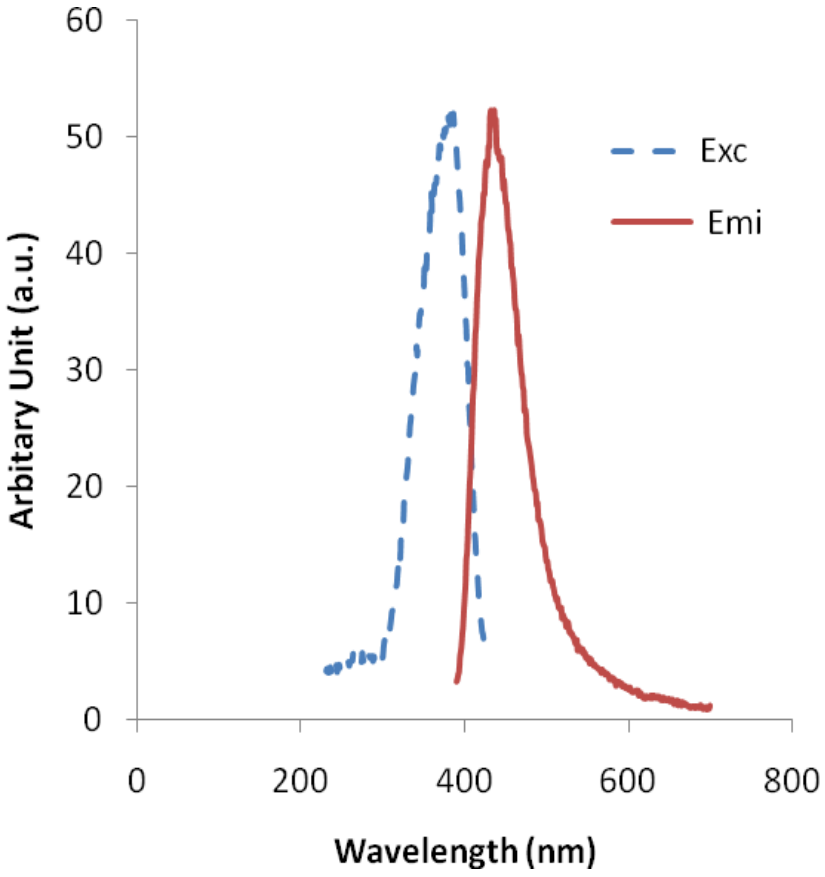

Fig 3.12: Excitation (blue) and emission spectra (red) for the porous scaffold of BPLP-cys prepared by using the salt leaching technique.

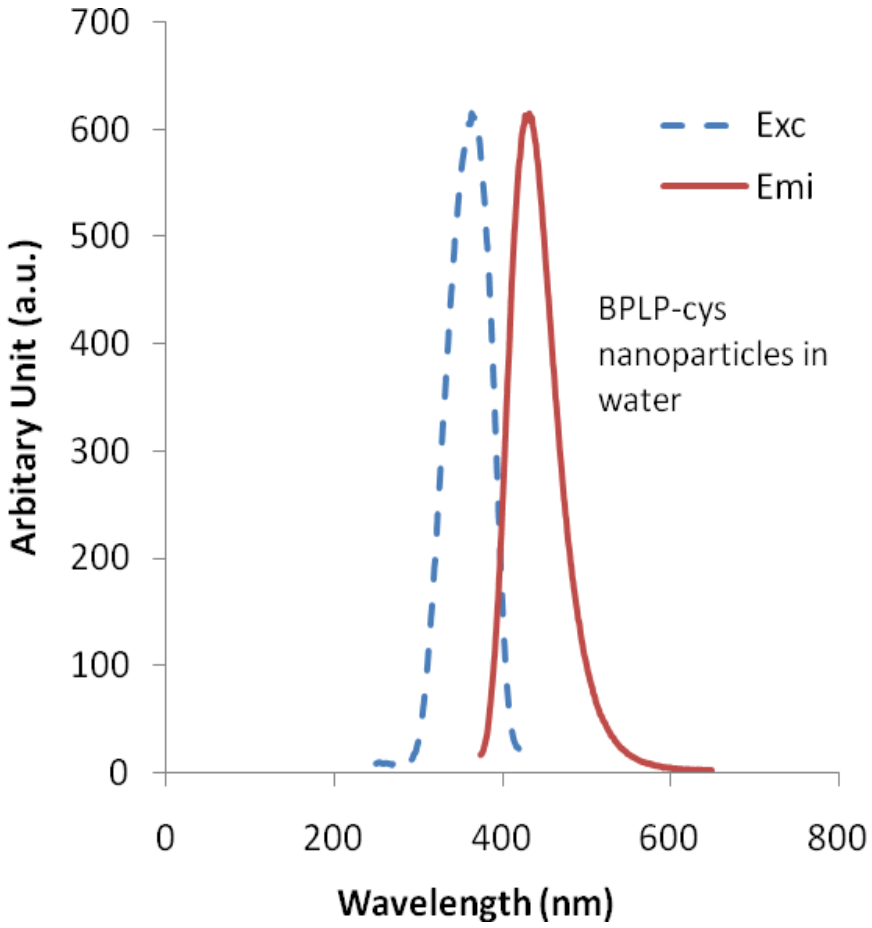

Fig 3.13: Excitation (blue) and emission spectra (red) for BPLP-cys nanoparticles prepared by nanoprecipitation technique

3.1.4.4 PL Study on the Effect of Concentration of BPLP-cys

To have a better understanding of the fluorescence properties, the effect of concentration of BPLP-cys was also studied. Figure 3.14 represents the spectra for various concentrations of polymers excited at 350 nm. With an increase in concentration of the polymer, the fluorescent intensity decreased and there was a slight red shift.

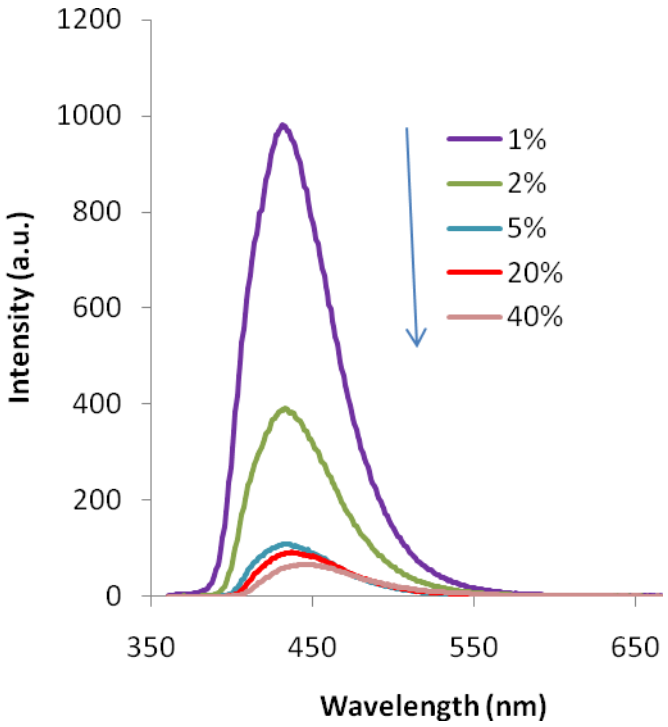

Fig 3.14: Emission spectra revealing the effect of concentration on the intensity of emission. BPLP-cys (0.4) was taken for this purpose.The samples with different concentrations by weight were prepared using 1,4 dioxane as a solvent.

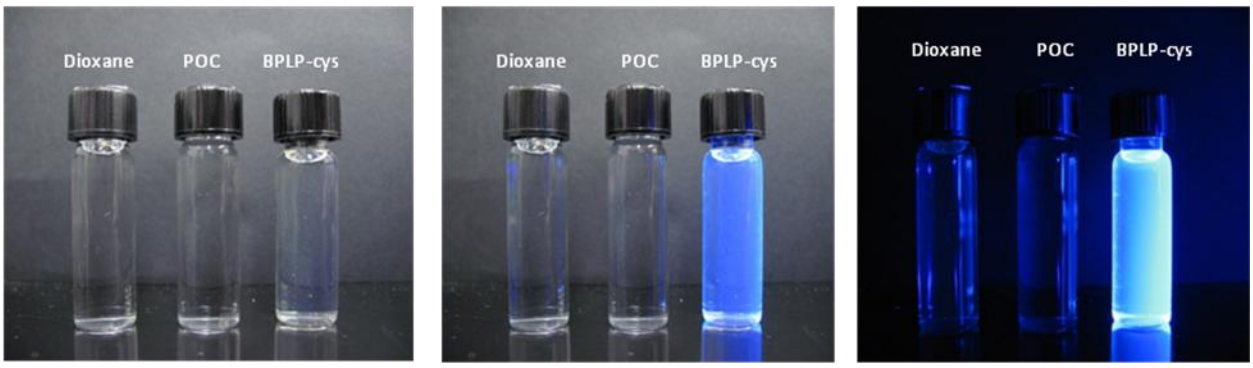

(A) (B) (C)

Fig 3.15: Photograph of BPLP-cys dissolved in 1,4-dioxane: A. Image in absence of UV light; B. Image under UV with room lights on; C. Image under UV in dark room. 1,4-dioxane and POC dissolved in dioxane were used as control.

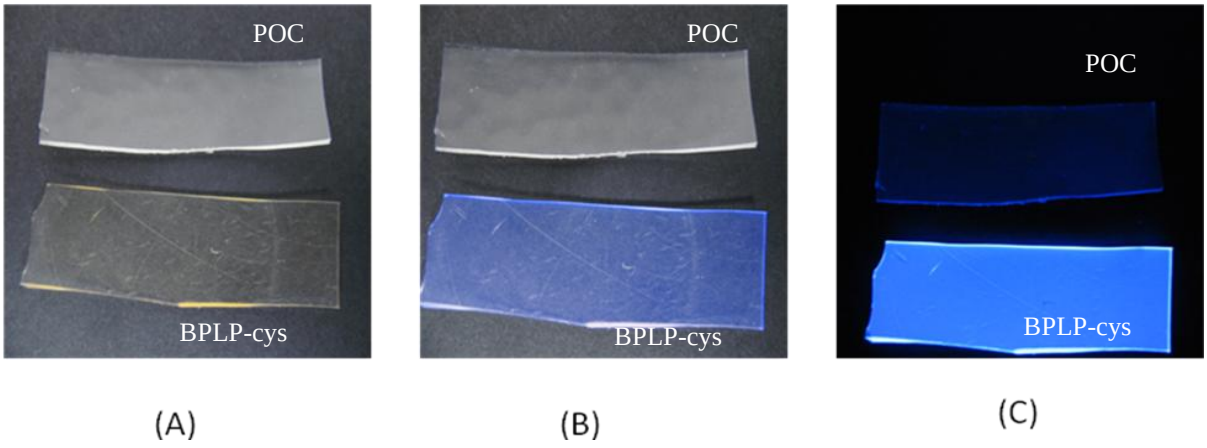

Fig 3.16: Photograph of POC and BPLP-cys polymer films post-polymerized at 80^0C for 4 days: A. Image in absence of UV light; B. Image under UV with room lights on; C. Image under UV in dark room. POC film was used as control.

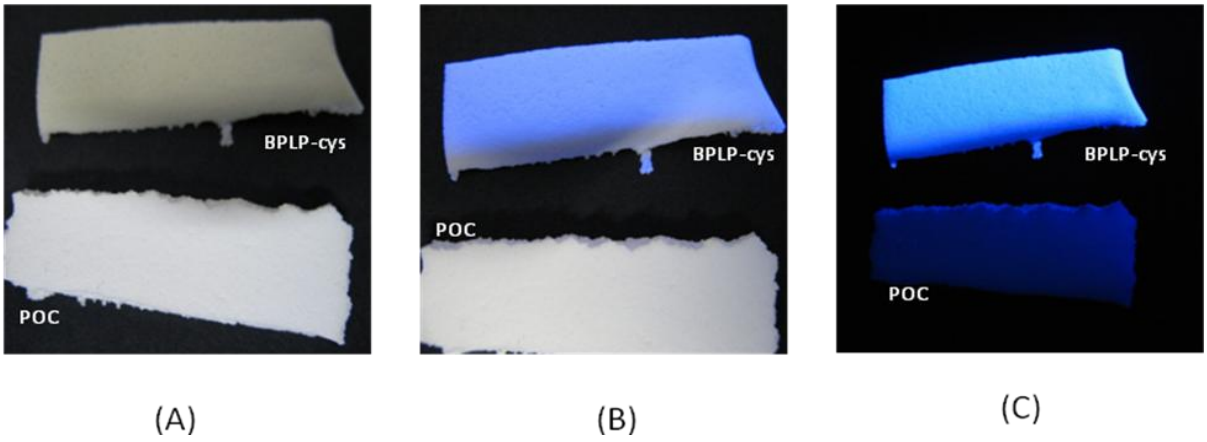

Fig 3.17: Photograph of salt leached scaffolds of POC and BPLP-cys: A. Image in absence of UV light; B. Image under UV with room lights on; C. Image under UV in dark room. POC scaffold was used as control.

3.1.5 Quantum Yield of BPLP-cys

Absorbance of BPLP-cys and Anthracene (standard) were plotted against their respective concentration as shown in figure 3.18. According to William's method, the slope of each solution is proportional to their quantum yield. The absolute quantum yield is calculated using equation (1). BPLP-cys has a high quantum yield of 0.58.

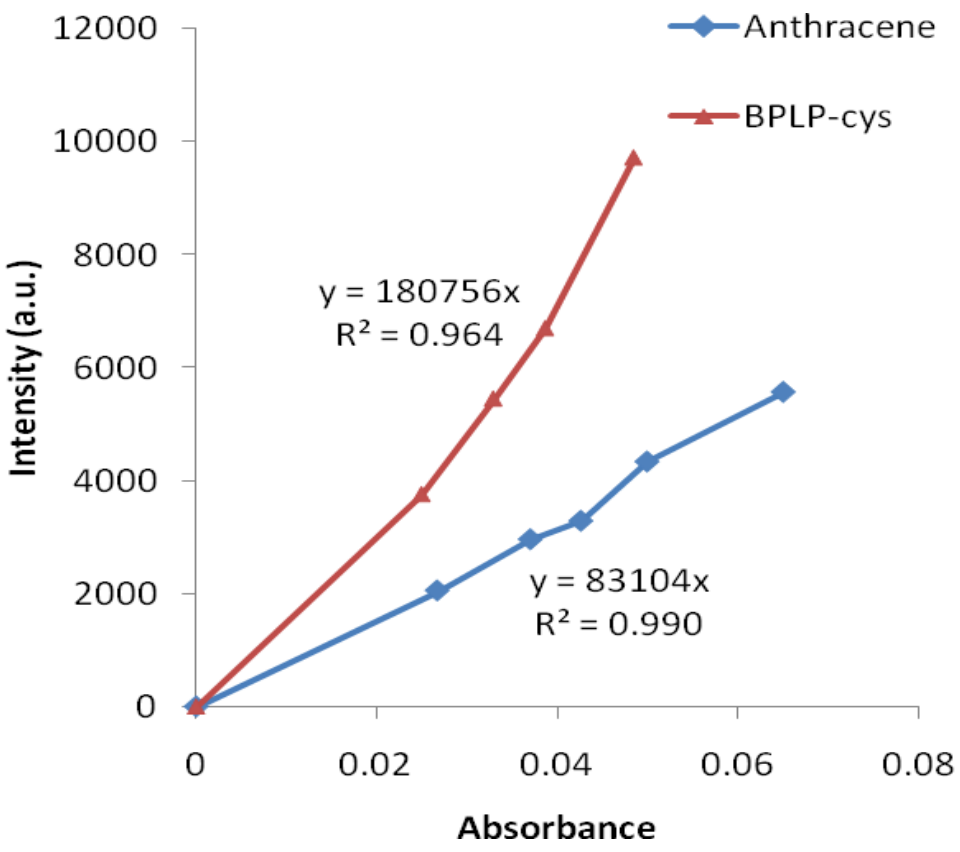

Fig 3.18: Linear plots of the standard (anthracene) and the sample (BPLP-cys 0.2) dissolved in ethanol to measure the quantum yield.

3.1.6 Lifetime of BPLP-cys

The fluorescent decay of BPLP-cys seemed exponential and it did not vary much for different ratios of cysteine. BPLP-cys (0.2) had a fluorescence lifetime of 10 ns whereas BPLP-cys (0.8) had 9.6 ns as shown in the figure 3.19.

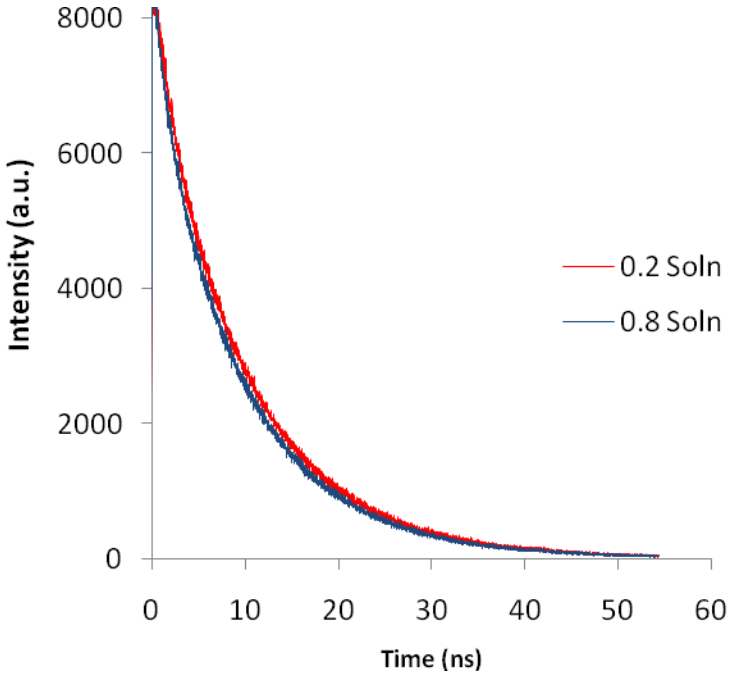

Fig 3.19: Fluorescence decay lifetime for two polymer samples dissolved in 1,4-dioxane using an excitation wavelength of 315 nm.

3.1.7 Mechanical Properties of BPLP-cys

Figure 3.20 shows the tensile strength and the Young's modulus of BPLP-cys polymers with different amount of cysteine incorporated in them. The tensile strength ranged from 3.25±0.13 MPa to 6.5±0.8 MPa whereas the Young's Modulus was in a range of 3.34±0.15 MPa to 7.02±1.40 MPa. It was found that the tensile strength and the modulus of BPLP-cys increased with an increased ratio of cysteine. So was the case of elongation. The maximum elongation was 240±36% (figure 3.21). The mechanical properties of BPLP-cys have been

summarized in Table 3.1. The specific density and the crosslinking density of those polymers increased with the amount of cysteine added.

Table 3.1: Mechanical properties of BPLPs with different ratios of cysteine in them.

Molar ratio of cysteine	Tensile Strength	Young's Modulus (MPa)	Elongation at break (%)	Density (g/cm^3)	n (mol/m^3)	M_c (g/mol)
0.2	3.2±0.13	3.34±0.15	139±10	1.20±0.013	454±21	2648±120
0.4	2.7±0.63	2.55±0.28	144±28	1.21±0.007	346±38	3536±371
0.6	3.6±0.60	3.83±0.53	162±34	1.22±0.013	597±71	2385±347
0.8	6.5±0.80	7.02±1.40	240±36	1.25±0.001	954±190	1351±255

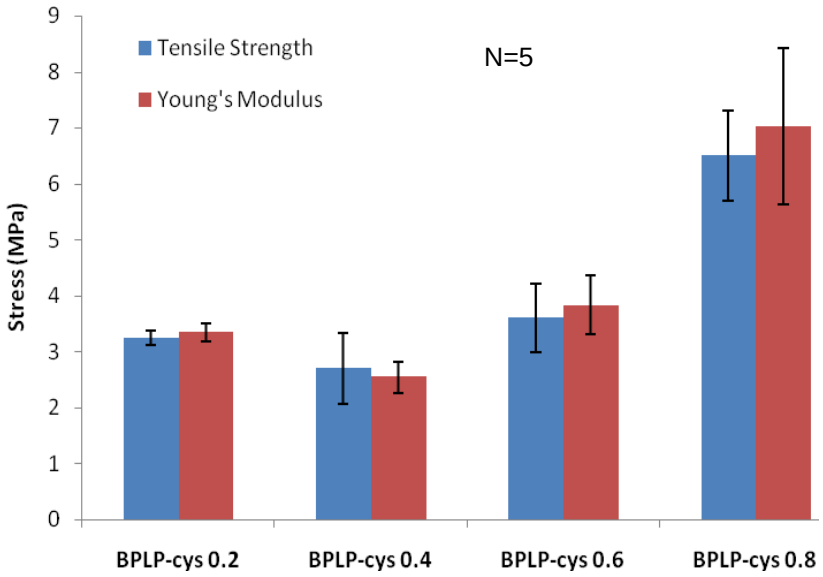

Fig 3.20: Comparision of tensile strength and Young's modulus of CBPLP-cys with four different ratios of cysteine incorporated into them.

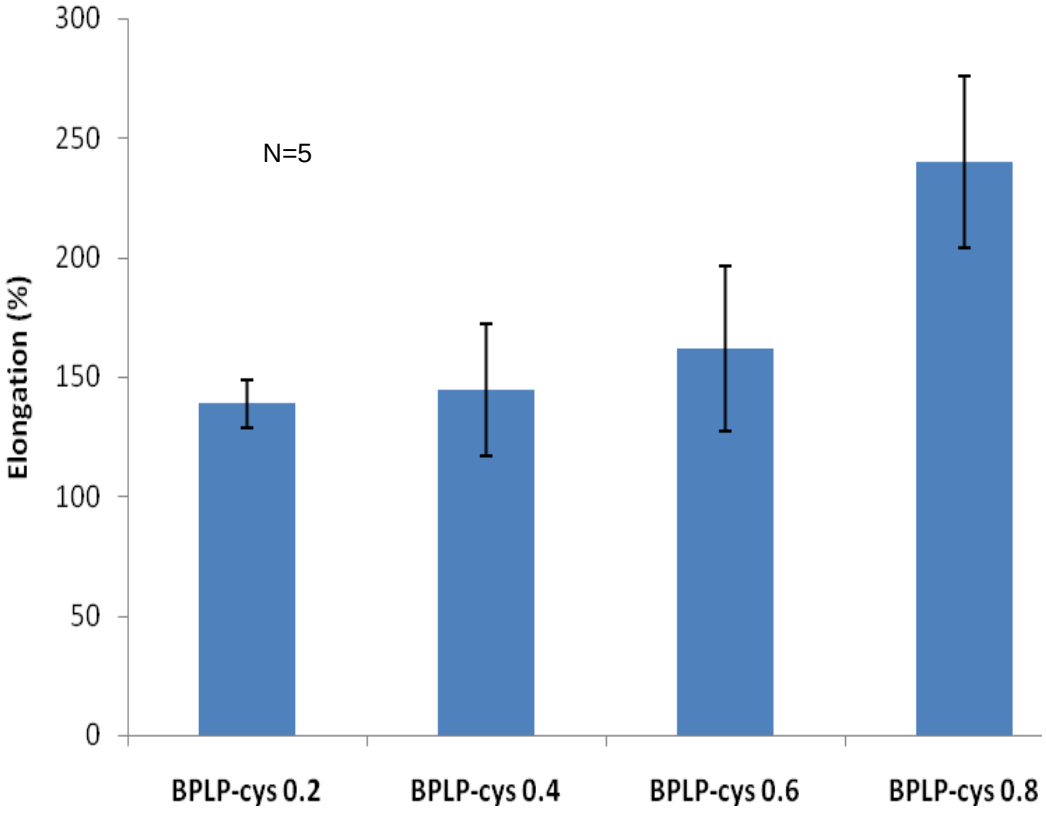

Fig 3.21: Comparision of elongation of CBPLP-cys with four different ratios of cysteine incorporated into them.

3.1.8 In Vitro Degradation Study

3.1.8.1 Degradation of BPLP-cys

The result of a pre-polymer degradation study is shown in Figure 3.22. With an increase in the amount of cysteine, the degradation rate also increased. Within 16 days, BPLP-cys with 0.6 molar ratio of cysteine degraded by almost 95%, whereas BPLP-cys with 0.2 molar ratio of cysteine degraded by 72%.

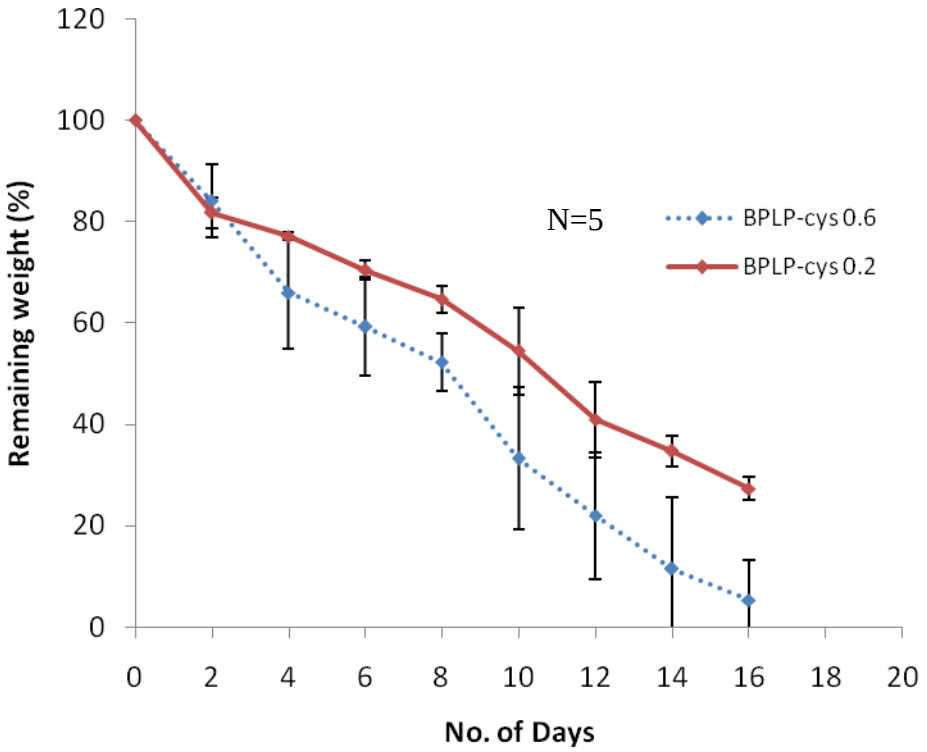

Fig 3.22: Results of in vitro pre-polymer degradation study. BPLP-cys (0.2) degraded about 72% after 16 days whereas BPLP-cys (0.6) degraded 95% in the same period of time.

3.1.8.2 PL Spectra of Degraded Samples

The results of the effect of degradation of the polymer on its fluorescence intensity is represented in figure 3.23. For BPLP-cys (0.2), the intensity of emission decreased steadily while the polymer was. The emission maxima was at the same position and the polymer was still intensely emitting even after a degradation of 72%. The result for the polymer with 0.6 cysteine showed an interesting trend. The intensity increased while the polymer degraded upto about 75%. After that, the intensity of fluorescence started to decrease. The intensity difference between the original sample and the sample that degraded upto 95% was not too large.

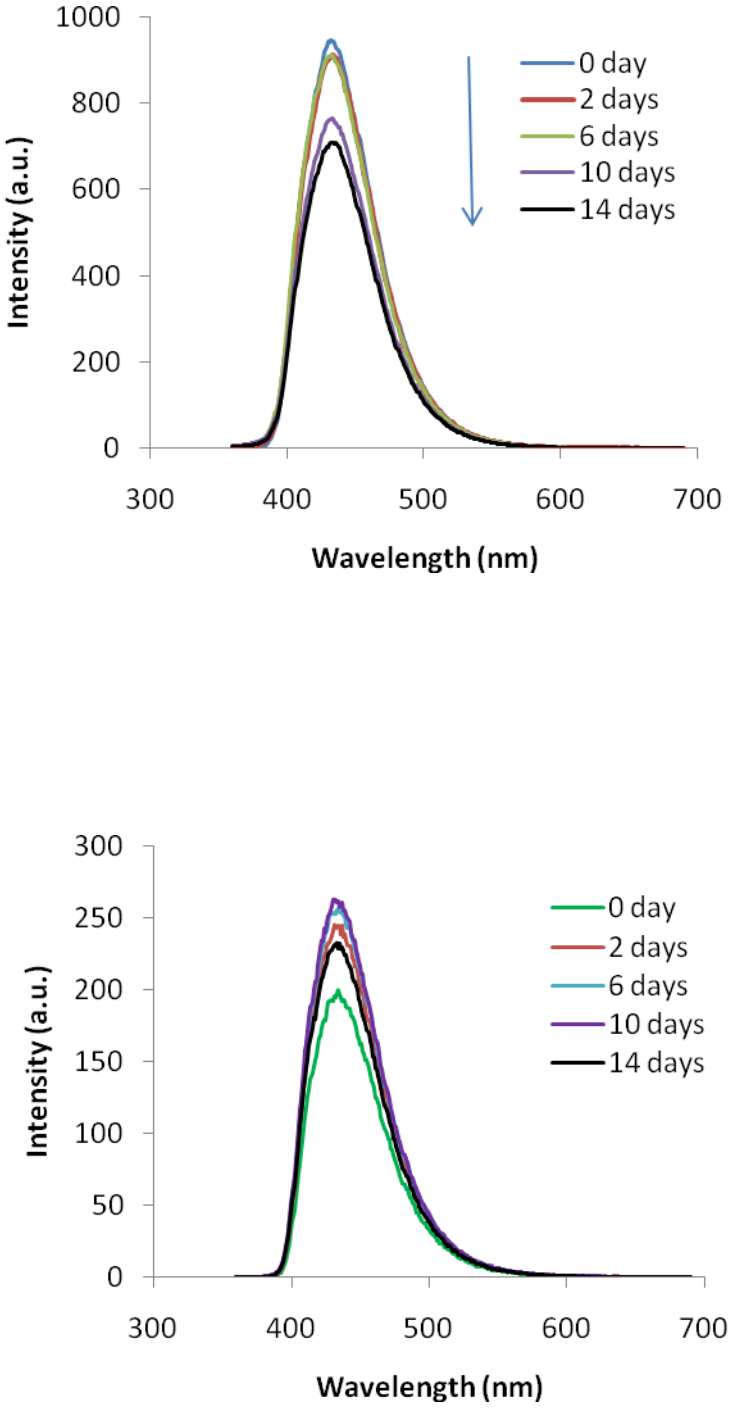

Fig 3.23: Effect of degradation of BPLP-cys on the fluorescent intensity. The plot on the top represents the polymer with 0.2 molar of cysteine whereas the bottom one represents the polymer with 0.6 molar of cysteine.

3.1.9 Cell Culture Study

In order to analyze the cytocompatibility of BPLP-cys, the 3T3 cells were grown both in CBPLP and BPLP-cys scaffold. The SEM image of the cells grown on CBPLP-cys showed the morphology of the confluent cells (figure 3.24).

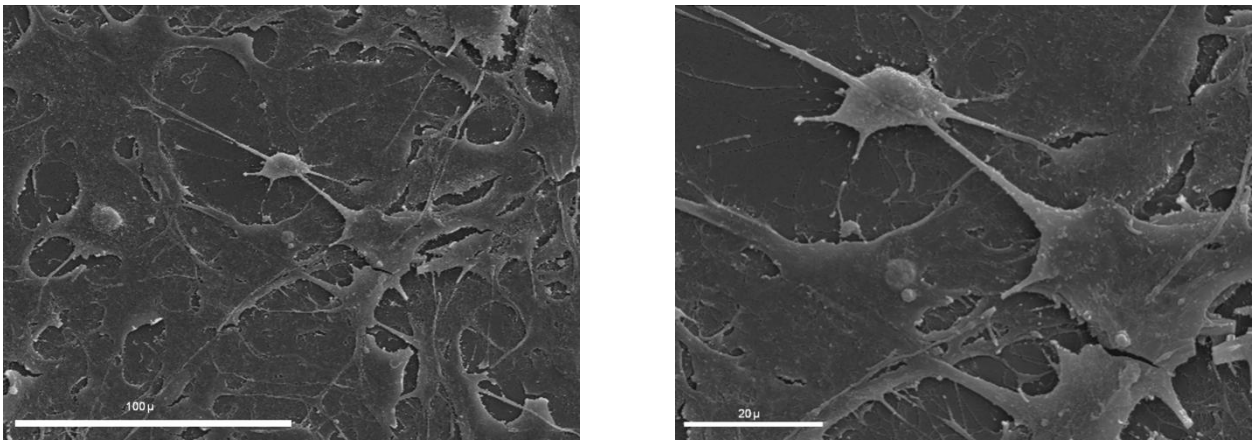

(a) (b)

Fig 3.24: SEM images depicting 3T3 fibroblasts growth and their morphology on CBPLP-cys surface. The scale on the left panel is 100 µm and on the right panel is 20 µm.

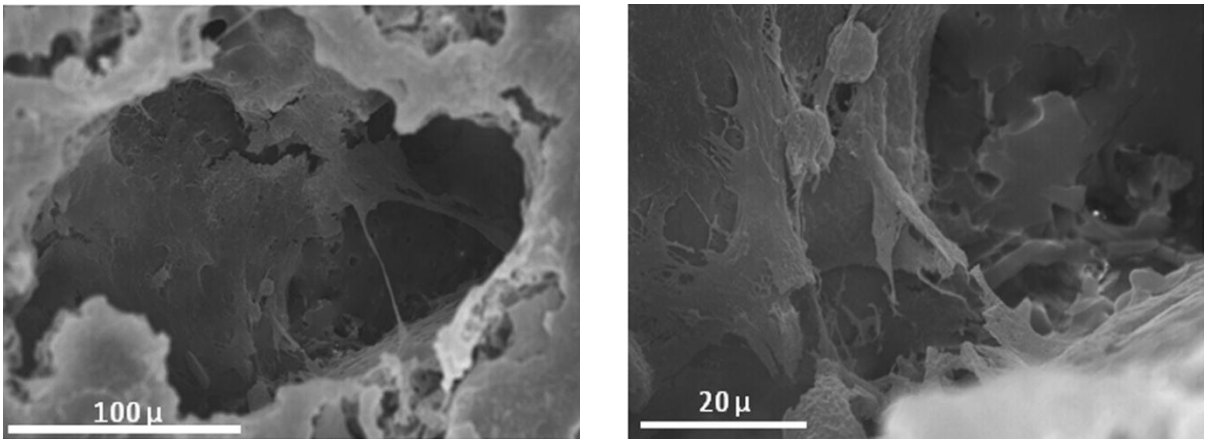

(a) (b)

Fig 3.25: SEM images of cross section of scaffolds show cellular infiltration into the pores of BPLP-cys scaffold. Images are taken at two separate magnifications. a. 500x b. 1200x

The SEM images of a cross section of BPLP-cys scaffold itself showed the interconnected pores, whereas a cross section of the cell seeded scaffold showed the cells were infiltrated into BPLP-cys scaffold (figure 3.25). The cells can be seen growing in the pore and along its edges.

3.1.9.1 H&E Staining

Figure 3.26 is a representative image of the H&E stained scaffold seeded with 3T3 cells. The purple colored nuclei of 3T3s are clearly visible. The infiltrated cells are spread throughout the scaffold. The clear spaces seen in between are the pores of the scaffold.

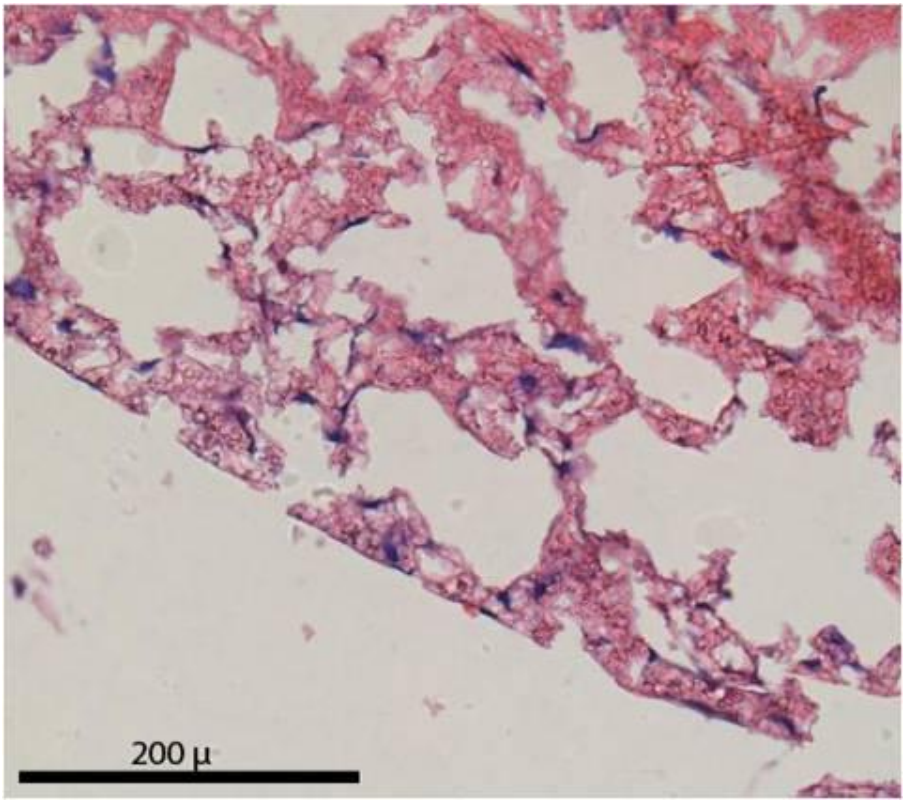

Fig 3.26: Cross sections of cell seeded scaffold (20 micron thick slices) were H&E stained and observed under a microscope at 20x. The presence of purple stained nuclei in the scaffold section indicated that the cells had attached and proliferated inside the scaffold.

3.1.10 Size and Distribution of Nanoparticles

3.1.10.1 Transmission Electron Microscopy

A representative TEM image of nanoparticles prepared by the nanoprecipitation technique is depicted below in figure 3.27. The nanoparticles were found to be uniformly distributed and well separated. They were more or less spherical in shape and their average size was around 75 nm as can be seen in the figure below. Nanoparticles prepared with low concentration or lower molar ratio of cysteine had smaller size of up to 50 nm. However, nanoparticles with a size of as high as 450 nm were obtained when high concentration of polymer was used.

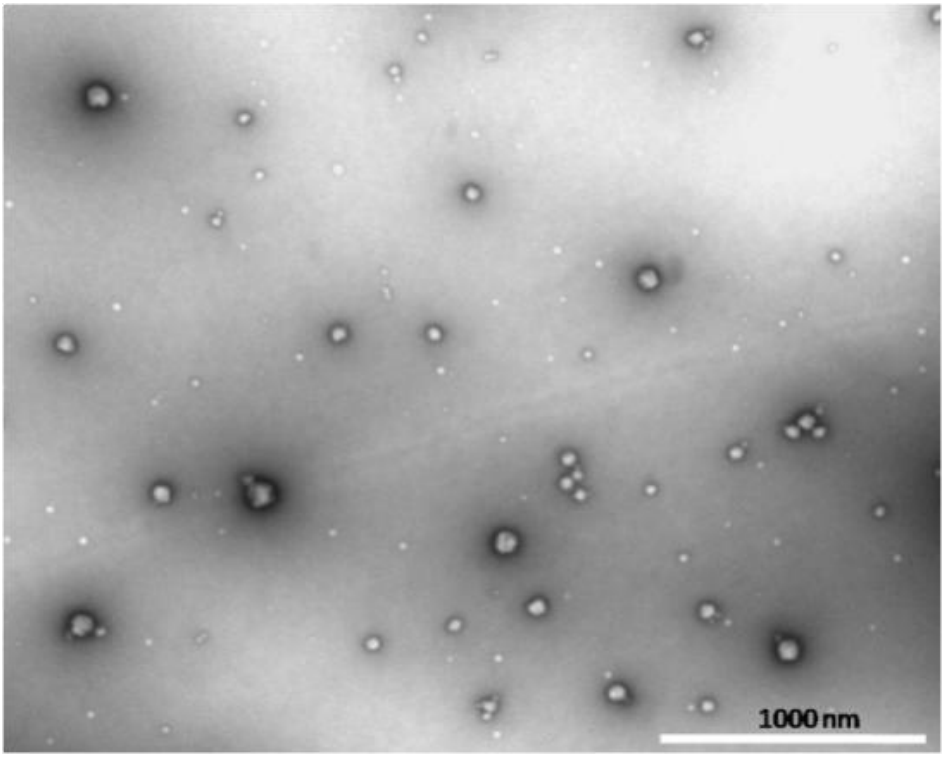

Fig 3.27: TEM image of nanoparticles prepared from BPLP-cys (0.2) has a size of 75 nm. Variation in size is achievable by either changing the concentration of the polymer or the molar ratio of cysteine in polymer.

3.1.10.2 Size and Distribution

To confirm the results obtained from TEM, DLS technology was used to observe the size and distribution of BPLP-cys nanoparticles (figure 3.28). The results showed an approximate size of 72 nm and the distribution was narrow.

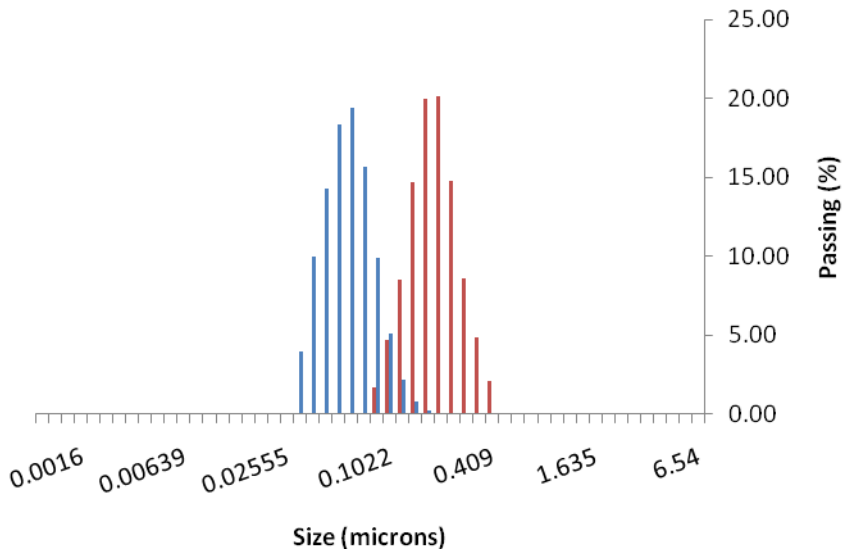

Fig 3.28: Size and distribution of BPLP-cys 0.2 nanoparticles prepared at two different concentrations. The size increased with concentration and the distribution of nanoparticles ranged from 50 nm to 450 nm.

3.2 Characterization of Water Soluble BPLP-PEG-cys

3.2.1 PL Spectra of Water-Soluble BPLP-PEG-cys

The PL spectrum of water soluble fluorescent polymer has an excitation maximum at 419 nm and emission maximum at 454 nm. A narrow excitation spectrum and a broad emission spectrum can be observed for the water soluble fluorescent polymer in figure 3.29.

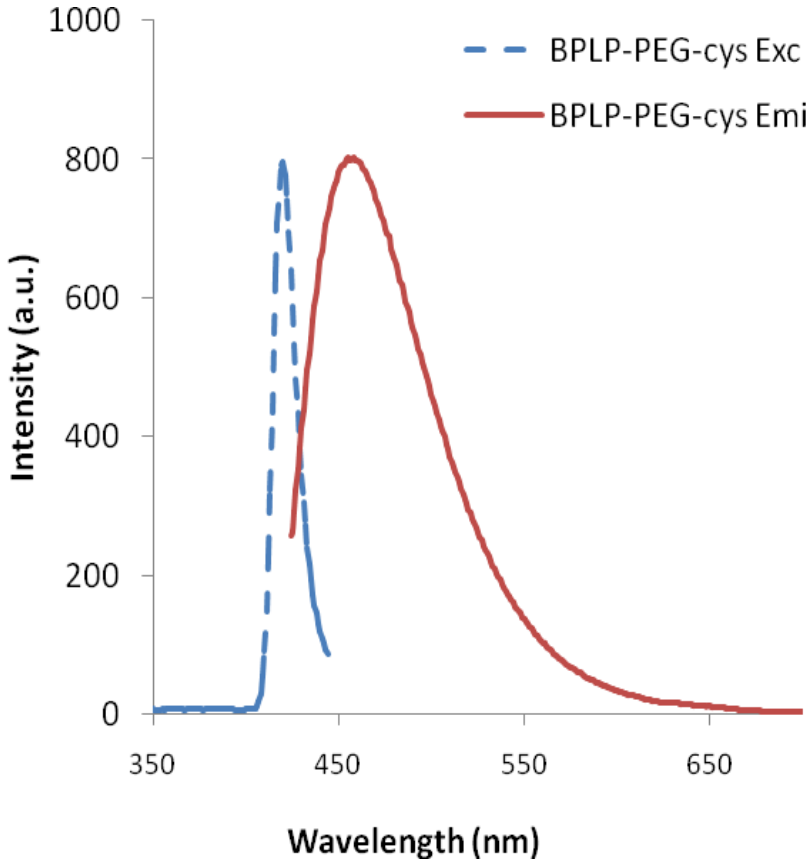

Fig 3.29: PL spectra for water soluble polymer shows a narrow excitation and a broad emission spectra. The slit width of 3/3 nm was used to take the measurement for this purpose.

3.3 Characterization of BPLPs with Other Amino Acids

In order to characterize their fluorescent properties, the polymers incorporated with rest of the other 19 amino acids were classified according to their polarity in order to observe if there is any co-relation among the fluorescence intensity and their polarity. There were nine amino acids with non-polar R-groups, six with polar R groups and five with charged R groups.

3.3.1 Absorbance of BPLPs Incorporated with Rest of the Amino Acids

The absorbance of polymers with each amino acid is presented in the figure below (figure 3.30 and figure 3.31). The absorbance of polar and charged amino acids showed a wide range of absorbance capability compared to the non-polar ones.

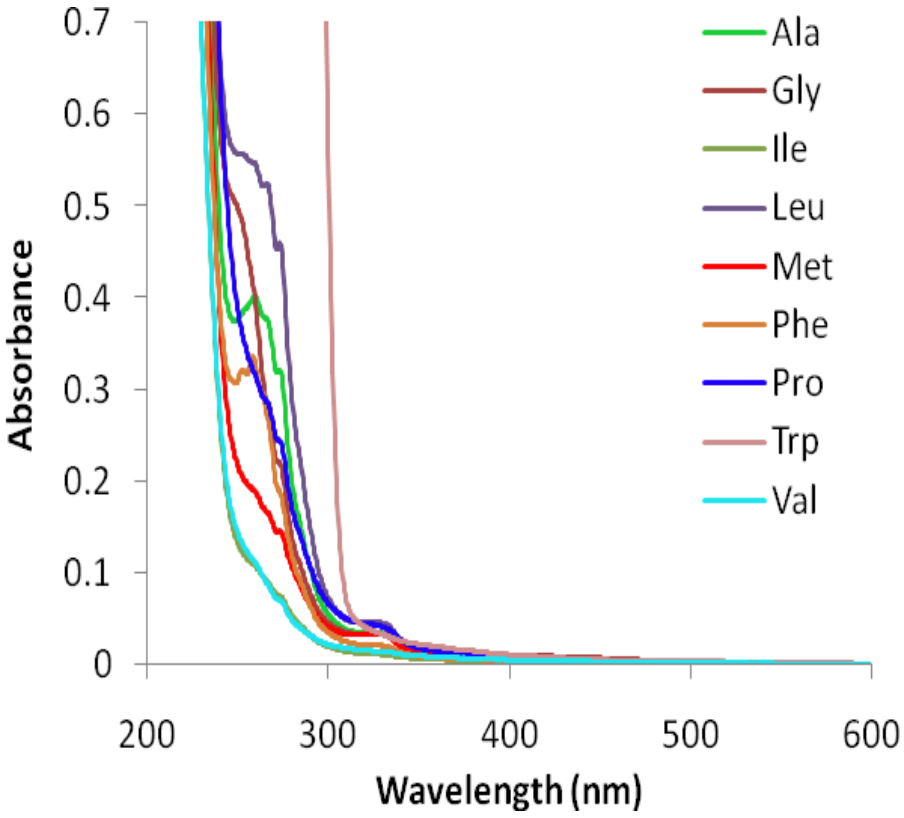

Fig 3.30 Absorbance spectra of the polymers incorporated with different amino acids containing non-polar R-groups. All the polymers were dissolved in 1,4 – Dioxane to make the solution of 1% concentration by weight.

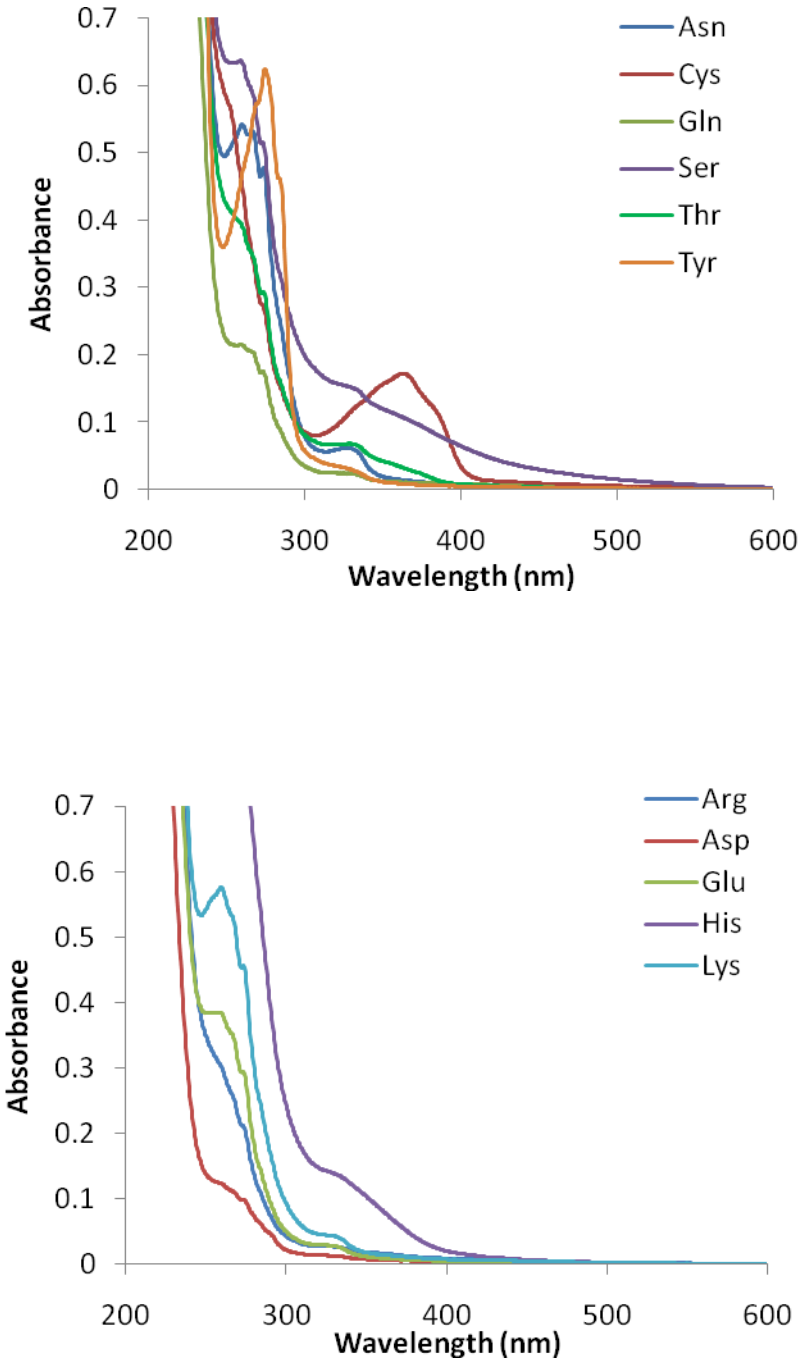

Fig 3.31: Absorption spectra for the polymers incorporated with the amino acids containing polar (top) and charged (bottom) R-groups. All the polymers were dissolved in 1,4 – Dioxane to make the solution of 1% concentration by weight.

3.3.2 PL Spectra of BPLPs Incorporated with Rest of the Amino Acids

The polymers were classified again in a similar fashion as it was mentioned for the absorbance. The polymers showed a capability of emitting light in a wide range of spectrum. With an increased excitation wavelength, the emission spectra shifted toward the red region of visible spectrum. Multiple spectra from the same polymer resulted in various peaks at different regions. The range where the peaks were observable are given in table 3.2.

Table 3.2: Excitation and the emission maxima range for BPLPs with various amino acids. All of them are photoluminescent and most of them emitted in the violet to blue region of the visible spectra.

	Non-polar groups			**Polar R Groups**			**Charged R Group**	
Name	*Exc (nm)*	*Emi (nm)*	*Name*	*Exc (nm)*	*Emi (nm)*	*Name*	*Exc (nm)*	*Emi (nm)*
Gly	265-510	314-557	Gln	280-500	356-554	Arg	250-503	312-537
Ala	250-413	310-471	Asn	280-490	312-548	His	310-540	382-580
Val	240-391	319-450	Cys	240-420	432-435	Lys	265-535	310-563
Pro	255-450	313-519	Tyr	240-440	362-507	Asp	275-415	322-477
Ile	250-403	310-460	Thr	250-470	359-516	Glu	255-415	415-474
Leu	275-415	315-481	Ser	290-580	319-608			
Met	250-396	321-454						
Phe	270-420	315-479						
Trp	300-490	365-545						

The emission of polymer with polar R-grouped amino acids was found to be more intense than rest of the amino acids. Cysteine also falls in the category of polar R-grouped amino acids which showed the highest intensity of emission.

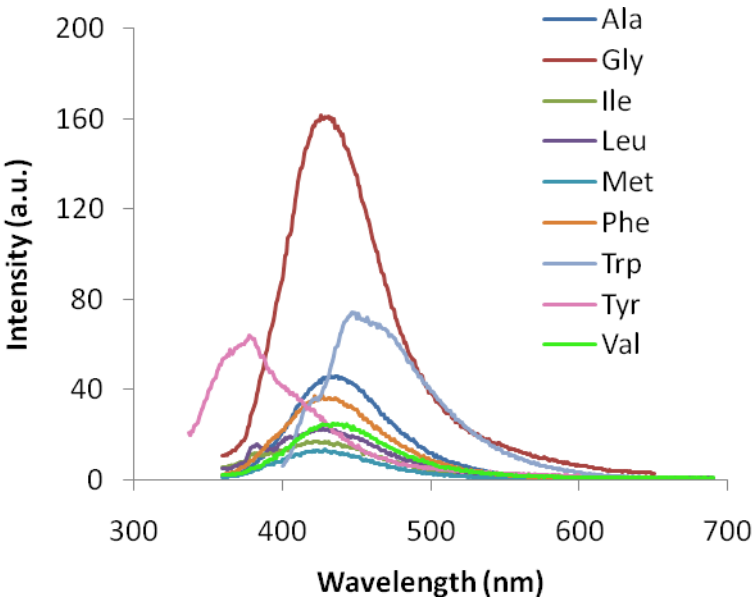

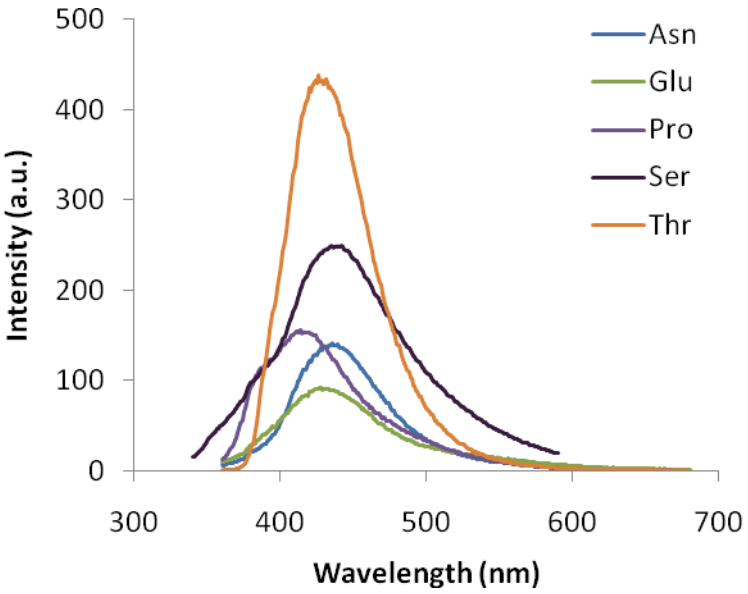

Fig 3.32: Emission spectra for the polymers incorporated with different amino acids containing non-polar R-groups (top) and polar R-groups (bottom). All the polymers were dissolved in 1,4 – Dioxane to make the solution of 5% concentration by weight.

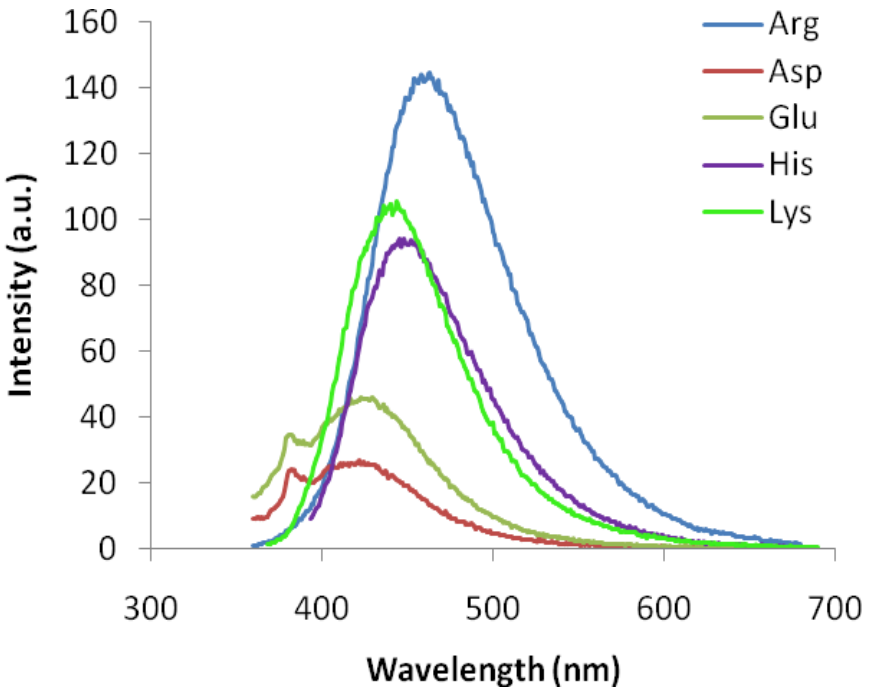

Fig 3.33: Emission spectra for the polymers incorporated with amino acids containing charged R-groups. All the polymers were dissolved in 1,4 – Dioxane to make the solution of 5% concentration by weight.

3.3.3 PL Spectra of BPLP-ser

The photoluminescent spectra of BPLP-ser emitted light of different colors of a visible spectrum. The color ranges from blue to orange as shown in figure 3.34. The intensity of emission decreased towards the red region of a visible spectrum. The results was obtained from a sample prepared in dixoane (5% w/w). The slit width was set at 3/3 nm. Similarly, photoluminescence spectra of the nanoparticles prepared from BPLP-ser is given in figure 3.35. A wide range of colors were also observed in some other amino acid incorporated polymers.

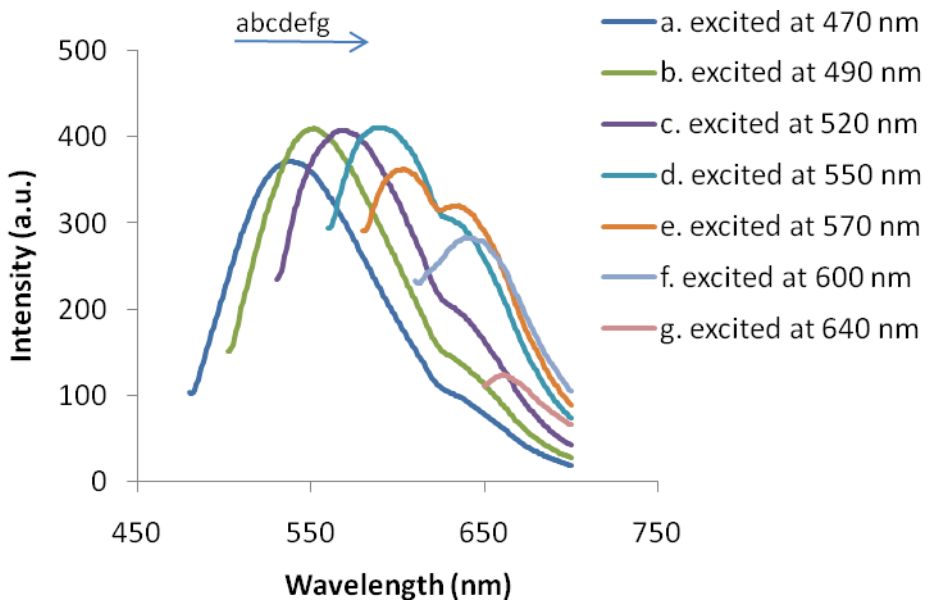

Fig 3.34: Emission spectra of BPLP-ser resulted from various excitation wavelengths.

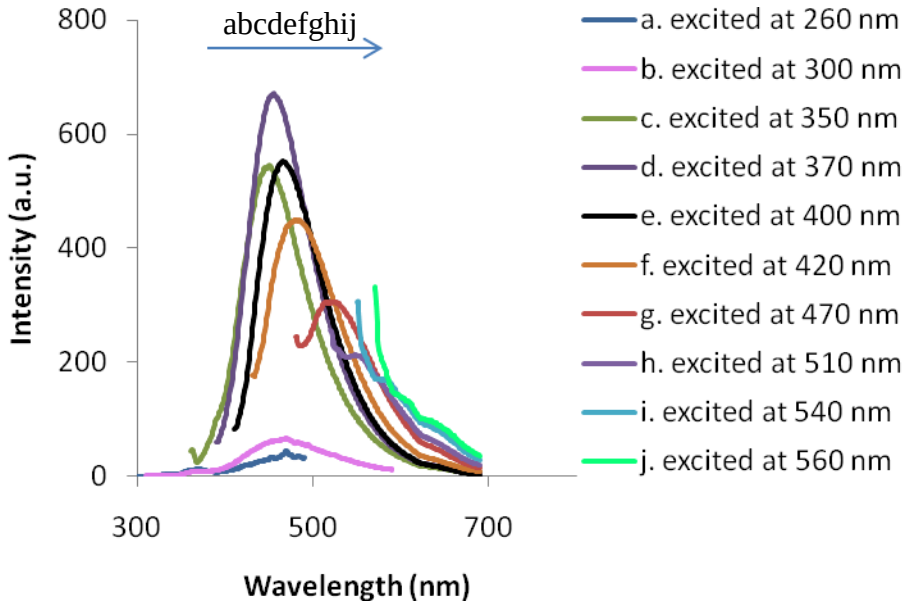

Fig 3.35: Emission spectra of nanoparticles prepared from BPLP-ser resulted from various excitation wavelengths.

CHAPTER 4

DISCUSSIONS

Examples of use of fluorescent polymers for tissue engineering purposes are rarely found. But, their applicability in tissue engineering should not be underestimated. Scaffolds fabricated from such polymers might provide a better understanding of tissue regeneration process by reducing the errors involved in scarification of multiple animals to understand a single process.

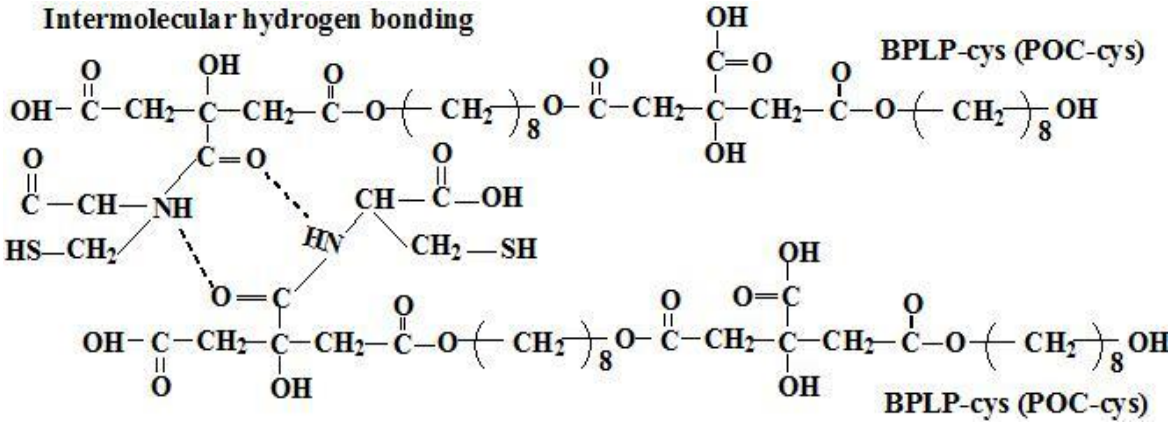

Fig 4.1 Hydrogen bonding between the chains of polymer forming conjugated system

The biodegradable fluorescent materials presented in this study have wide range of flexibility in terms of size, fluorescence and other mechanical properties. These properties can be utilized for multiple scientific purposes. Various characterizations revealed that the BPLPs

were composed of three dimensional network of polyester formed by reaction of citric acid, octanediol and cysteine. The reason behind the fluorescence of BPLPs was attributed to the conjugated structure that is formed due to hydrogen bonding between two chains of the polymer. The schematic diagram of BPLPs ability to form a conjugated system by hydrogen bonding is revealed in figure 4.1. Fluorescence that results from the formation of conjugated system due to hydrogen bonding has been previously reported [57].

The hydroxyl, alkane and carbonyl groups observed from FTIR spectrum confirmed the presence of octanediol and citric acid in the pre-polymer. In addition to those groups, FTIR spectrum also shows the thiol and the amide groups. It indicated the incorporation of cysteine into the base polymer poly (1,8-Octanediol Citrate) (POC).

The inverse relationship between absorbance of cysteine and its concentration might be due to quenching of the fluorescence, self-quenching in particular. Self quenching results when there are formation of trap sites and energy transfer among fluorophores which will bring the possibility of trap sites migration and quenching subsequently [58]. Addition of more cysteine into the polymer chain might result in the more trap site formation and increased quenching. There was a red shift in spectra of films from the spectra of solution. It can be attributed to the aggregation phenomenon in the solid phase [59,60]. A small red shift also indicated that polymeric films and solutions do not have much of a molecular conformation change [3]. The decrease in fluorescent intensity with an increased amount of cysteine or increased concentration of polymer is due to self quenching which has been already described earlier. There was a slight red shift of spectra while the amount of cysteine or concentration of polymer was increased. It was due to the aggregation phenomena which depends on concentration of the polymer and the solvent system [61].

The intensity of emission reduced abruptly in the BPLP-cys scaffolds. It could be due to the lack of intact structure of scaffold. The porous form of the scaffold means widely separated lesser number of fluorophores which resulted in lesser emission intensity. The intensity of

emission for BPLP-cys nanoparticles was slightly lower than that of polymer solution or film. It might be because of lesser fluorophores that are present in the nanoparticles than that of the polymer. Only 10mg of polymer was taken and precipitated in 100mL of water to make the nanoparticles. That means there is a vast reduction in the numbers of fluorophores that are present in the nanoparticles solution than in the polymeric solution/film. This reduction might play a role in the decreased intensity of nanoparticles. A shift of only 1nm and 2nm in the emission spectra for the scaffold and the nanoparticles respectively confirms that they have similar molecular confirmation that of the polymer.

The quantum yield is considered an essential parameter in the selection of fluorescent related applications [62]. For LEDs, flat panel displays and other imaging applications, higher quantum yield is always desirable to get the better resolution. The quantum yield of 0.58 for BPLP-cys polymer is much higher than the quantum yield of common green fluorescent proteins like the wild type blue (QY 0.079) and green fluorescent protein (QY 0.073) extracted from *Aequoria* [63]. However, the quantum yield of the genetically engineered variants of the same species have relatively higher quantum yield. The quantum yield of green color variant of *Aequoria* (EGFP) (QY 0.6) and yellow variant of *Aequoria* (EYFP) (QY 0.61) are comparable to that of BPLP-cys [64]. However, quantum yield of other genetically engineered cyan color variant of *Aequoria* (ECFP) (QY 0.4) and blue color variant of *Aequoria* (EBFP) (QY 0.25) are much less than that of BPLP-cys [64]. Compared to GFPs, the other variants undergo rapid photobleaching [64]. The utility of most of the blue fluorescent proteins is still questionable because they suffer from low quantum yield and rapid photobleaching [65] hence, reducing their utility. BPLP-cys with high quantum yield can possibly be a better alternative to blue fluorescent proteins.

The fluorescence lifetime of fluorescent compounds is another useful criterion generally used in the selection of materials for imaging applications. A longer lifetime is desirable for applications like fluorescence lifetime imaging microscopy (FLIM). Commonly known fluorescent

dyes and fluorescent proteins have their lifetime in a range of picoseconds to a couple of nanoseconds. The fluorescence lifetime of different variants of GFPs are found to be in the range of 1.3-3.7 ns [66, 67]. A well known fluorescent dye, rhodamine 6G has a fluorescence lifetime in a range of 0.5-4 ns [68]. The fluorescence lifetime of BPLP-cys reported here was as high as 10 ns which is much longer than the range of conventional dyes and GFPs. Longer lifetime speaks for its potential in imaging related applications.

The crosslinking density of CBPLP-cys increased with an increasing amount of cysteine in the polymer. The chance of formation of crosslink is always higher with the availability of extra cysteine because of carboxylic and amine functional groups in it. The polymer becomes more intact with increased crosslinking, hence increasing the density of polymers. The tensile strength and elongation of the polymer is comparable to the mechanical properties of soft tissues [55]. Polymers with a range of tensile strength, Young's modulus and elongation can be created by changing the ratio of reactants and can be used for several soft tissue engineering purposes. The mechanical properties of elastomeric BPLPs support these polymers can be used as materials for tissue engineering applications, especially for soft tissue engineering applications.

Amide bonds and esters bonds are commonly known hydrolyzable groups. The rate of hydrolysis increases with the amount of such groups present in both the backbone and the side chain [47]. Enhanced hydrolysis means faster degradation rate. Addition of cysteine increases the number of both amide and esters bond in the polymer hence making it more susceptible to hydrolysis. The rate of degradation can be controlled through a variation of amount of cysteine. The higher percentage of degradation shown here was just for pre-polymer (BPLP-cys). The crosslinked polymer (CBPLP-cys) degradation is expected to be much longer because of the availability of multiple functional groups that have a potential to form crosslinks. The degradation rates for polymers, however, can actually be manipulated by changing the ratio of reactants and postpolymerization conditions.

The SEM images on both the films and the scaffolds showed that the polymer supports the cell attachment and growth. The H&E stained images of the scaffold seeded with cells also showed the proliferated single layered 3T3s on the scaffold surface. These facts suggest that the polymeric material is cell-friendly. The cell-friendly nature of the polymer makes a strong case for its potential in tissue engineering.

The TEM image of the BPLP-cys nanoparticles showed uniformly distributed and identical sized nanoparticles. The size and distribution of the polymer nanoparticles were also confirmed by using DLS. The uniformity and small size of the nanoparticles are considered to be important factors for cellular uptake and tissue targeting [69]. The concentration and molar ratio of cysteine can be changed to adjust the size of the nanoparticles. The variety in size and its fluorescent properties can be combined to tag different macromolecules and cells itself.

A narrow excitation and broad emission spectra of the water soluble polymer could be due to the extended π-conjugation range [70]. Such features are commonly found in the fluorescent dyes and fluorescent proteins. So, the polymer can be excited within a very small range of wavelength. A broad emission spectrum also means a lack of color purity. Despite of these disadvantages, the water soluble polymer is superior to the quantum dots in terms of cytotoxicity and degradability. Water soluble BPLP polymers, which are comparatively cheaper, can be used in multiple applications as an alternative to the common fluorescent dyes and the fluorescent proteins as well. With the incorporation of various amino acids, it was also shown that the polymers were capable of emitting lights of different colors. This makes them a useful probe for multi-color imaging applications.

CHAPTER 5

CONCLUSIONS

In this research project, a family of biodegradable fluorescent polymers was successfully synthesized. The structure and properties of this novel class of polymer was characterized using various techniques. The polymers were readily soluble either in organic solvents or in water. They could be easily processed into film, scaffold and nanoparticles using simple common methods. A wide range of mechanical properties of the polymeric films were comparable to some of the soft tissues. The biodegradation of the polymers was demonstrated by in vitro degradation study whereas their cytocompatibility was verified by in vitro cell culture study. The biocompatibility, degradability and controllable mechanical properties of polymers sum up for their potential applicability for tissue engineering designs. In addition to these properties, the fluorescent properties of polymer solution, film, scaffold and nanoparticles were determined using UV-vis spectrophotometer, fluorospectrophotometer and lifetime study. Higher quantum yield and longer fluorescent lifetime of BPLPs compared to the conventional dyes make them a better choice in fluorescent related applications. The amine groups found in a side chain could be used to conjugate nanoparticles with various molecules as a drug delivery vehicle. The size and morphology of nanoparticles were determined by dynamic light scattering technology (Nanotrac). The size of nanoparticles could be easily controlled by changing the concentration of the polymer used to prepare them. A wide range of applications can be achieved through a variation in size. Such nanoparticles have a potential application in the area of bioimaging. Similarly, the BPLPs synthesized using other amino acids show emission in various regions of the visible spectrum. Optimizing their color might be a helpful tool for multi-

color imaging applications. In overall, this study demonstrated that a family of biodegradable and biocompatible polymers with controllable mechanical and fluorescent properties can be synthesized using simple methods and they carry a promising future in biology and biomedical engineering related applications.

CHAPTER 6

LIMITATIONS AND FUTURE WORK

The application of those polymers might be limited due to their inability to emit light of equal intensity in all regions of the visible spectrum. For example, although BPLP-cys has high quantum efficiency, it only emits light in blue region of visible spectrum. Other polymers of this family emit very intense light in blue region which gradually decreases when red shifted. A spectrum that is generally broader than the ones from quantum dots might limit their role in applications that might need purity of color. The use of nanoparticles might be limited due to their tendency to aggregate. Aggregation of nanoparticles has been reported in other literatures too and can be reduced either by sonication or preparing fresh samples before using them.

The future work on BPLPs can be done in the area of color tuning. The nanoparticles can be conjugated with other molecules and their possibility as drug delivery vehicle can be investigated. The in vivo implantation study might be a necessary step to further assure the biocompatibility of polymers. Investigating the possibility of in vivo imaging can be done by injecting polymer solution or nanoparticles into animals.

REFERENCES

1. Zheng J, Zhan C, Wu S, Zhou L, Yang X, Zhan R, Qin J. *A highly soluble blue light emitting copolymer of anthracene and dialkyloxyl benzene prepared by oxidative-coupling reaction.* Polymer, 2002. **43**(6): p. 1761-1765.
2. Deimede V, Kallitsis JK, Pakula T. *Synthesis and properties of amorphous blue-light-emitting polymers with high glass-transition temperatures.* Journal of Polymer Science Part A Polymer Chemistry, 2001. **39**(18): p. 3168-3179.
3. Wang E, Li C, Peng J, Cao Y. *High-efficiency blue light-emitting polymers based on 3, 6-silafluorene and 2, 7-silafluorene.* Journal of Polymer Science Part B: Polymer Physics, 2007. **45**(21): p. 4941-4949.
4. Huang SP, Huang GS, Chen SA. *Deep blue electroluminescent phenylene-based polymers.* Synthetic Metals, 2007. **157**(21): p. 863-871.
5. Kobayashi N, Kijima M. *Blue electroluminescent properties of poly (N-arylcarbazole-2, 7-ylene) homopolymers.* Applied Physics Letters, 2007. **91**: p. 081113.
6. Mikroyannidis JA. *Synthesis and characterization of soluble, photoluminescent polyamides, polyesters and polyethers containing 9, 10-di (4-biphenylyl) anthracene segments in the main chain.* Polymer, 2000. **41**(23): p. 8193-8204.
7. Barashkov NN, Gunder OA. *Fluorescent polymers*. 1994: Ellis Horwood.
8. Yasuda T, Namekawa K, Iijima T, Yamamoto T. *New luminescent 1, 2, 4-triazole/thiophene alternating copolymers: Synthesis, characterization, and optical properties.* Polymer, 2007. **48**(15): p. 4375-4384.
9. Alimi K, Molinie P, Blel N, Fave JL, Bernede JC, Ghedira M. *Synthesis and characterization of C1–4poly-phenylene-vinylene–ether photoluminescent copolymers.* Synthetic Metals, 2002. **126**(1): p. 19-25.

10. Feldman D, Barbalata A. *Synthetic polymers: Technology, properties, applications*. 1996: Kluwer Academic Publishers.

11. Szycher M. *Szycher's handbook of polyurethanes*. 1999: CRC Press.

12. Burroughes JH, Bradley DDC, Brown AR, Marks RN, Mackay K, Friend RH, Burns PL, Holmes AB, *Light-emitting diodes based on conjugated polymers*. Nature,1990. **347** p. 539-541.

13. Yang Z, Sokolik I, Karasz FE. *A soluble blue-light-emitting polymer.* Macromolecules, 1993. **26**: p. 1188-1190.

14. Kim DY, Cho HN, Kim CY. *Blue light emitting polymers.* Progress in Polymer Science, 2000. **25**(8): p. 1089-1139.

15. Zollinger H. *Color chemistry: Syntheses, properties, and applications of organic dyes and pigments*. 2003: Wiley-VCH.

16. Thompson RB. *Fluorescence sensors and biosensors*. 2006: CRC/Taylor & Francis.

17. Lavis LD, Raines RT. *Bright ideas for chemical biology.* ACS Chemical Biology, 2008. **3**(3): p. 142-55.

18. Jamieson T, Bakhshi R, Petrova D, Pocock R, Imani M, Seifalian AM. *Biological applications of quantum dots.* Biomaterials, 2007. **28**(31): p. 4717-32.

19. Zimmer M. *Glowing genes : A revolution in biotechnology*. 2005: Prometheus Books.

20. Jaiswal JK, Mattoussi H, Mauro JM, Simon SM. *Long-term multiple color imaging of live cells using quantum dot bioconjugates.* Nature Biotechnology, 2003. **21**(1): p. 47-51.

21. Gao X, Yang L, Petros JA, Marshall FF, Simons JW, Nie S. *In vivo molecular and cellular imaging with quantum dots.* Current Opinion in Biotechnology, 2005. **16**(1): p. 63-72.

22. Chen W. *Nanoparticle fluorescence based technology for biological applications.* Journal of Nanoscience and Nanotechnology, 2008. **8**(3): p. 1019-51.

23. Tsien RY. *The green fluorescent protein.* Annual Review of Biochemistry, 1998. **67**: p. 509-44.

24. Mauring K, Krasnenko V, Miller S. *Photophysics of the blue fluorescent protein.* Journal of Luminescence, 2007. **122**: p. 291-293.

25. Heim R, Tsien RY. *Engineering green fluorescent protein for improved brightness, longer wavelengths and fluorescence resonance energy transfer.* Current Biology, 1996. **6**(2): p. 178-82.

26. Mena MA, Treynor TP, Mayo SL, Daugherty PS. *Blue fluorescent proteins with enhanced brightness and photostability from a structurally targeted library.* Nature Biotechnology, 2006. **24**(12): p. 1569-71.

27. Miyawaki A, Sawano A, Kogure T. *Lighting up cells: Labelling proteins with fluorophores.* Nature Cell Biology, 2003. **Suppl**: p. S1-7.

28. March JC, Rao G, Bentley WE. *Biotechnological applications of green fluorescent protein.* Applied Microbiology and Biotechnology, 2003. **62**(4): p. 303-15.

29. Michalet X, Pinaud FF, Bentolila LA, Tsay JM, Doose S, Li JJ, Sundaresan G, Wu AM, Gambhir SS, Weiss S. *Quantum dots for live cells, in vivo imaging, and diagnostics.* Science, 2005. **307**(5709): p. 538-44.

30. Su J, Zhang J, Liu L, Huang Y, Mason RP. *Exploring feasibility of multicolored cdte quantum dots for in vitro and in vivo fluorescent imaging.* Journal of Nanoscience and Nanotechnology, 2008. **8**(3): p. 1174-7.

31. Pinaud F, Michalet X, Bentolila LA, Tsay JM, Doose S, Li JJ, Iyer G, Weiss S. *Advances in fluorescence imaging with quantum dot bio-probes.* Biomaterials, 2006. **27**(9): p. 1679-87.

32. Xing B, Li W, Sun K. *A novel synthesis of high quality cdte quantum dots with good thermal stability.* Materials Letters, 2008. **62**(17-18): p. 3178-3180.

33. Li H, Shih WY, Shih WH. *Non-heavy-metal ZnS quantum dots with bright blue photoluminescence by a one-step aqueous synthesis.* Nanotechnology, 2007. **18**(20): p. 205604-1.

34. Chan WC, Maxwell DJ, Gao X, Bailey RE, Han M, Nie S. *Luminescent quantum dots for multiplexed biological detection and imaging.* Current Opinion in Biotechnology, 2002. **13**(1): p. 40-6.

35. Fan TW, Teh SJ, Hinton DE, Higashi RM. *Selenium biotransformations into proteinaceous forms by foodweb organisms of selenium-laden drainage waters in california.* Aquatic Toxicology, 2002. **57**(1-2): p. 65-84.

36. Hamilton SJ. *Review of selenium toxicity in the aquatic food chain.* Science of the Total Environment, 2004. **326**(1-3): p. 1-31.

37. Kondoh M, Araragi S, Sato K, Higashimoto M, Takiguchi M, Sato M. *Cadmium induces apoptosis partly via caspase-9 activation in HL-60 cells.* Toxicology, 2002. **170**(1-2): p. 111-7.

38. Derfus AM, Chan WCW, Bhatia SN. *Probing the cytotoxicity of semiconductor quantum dots.* Nano Letters, 2004. **4**(1): p. 11.

39. Lovric J, Bazzi HS, Cuie Y, Fortin GR, Winnik FM, Maysinger D. *Differences in subcellular distribution and toxicity of green and red emitting cdte quantum dots.* Journal of Molecular Medicine, 2005. **83**(5): p. 377-85.

40. Clarke SJ, Hollmann CA, Zhang Z, Suffern D, Bradforth SE, Dimitrijevic NM, Minarik WG, Nadeau JL. *Photophysics of dopamine-modified quantum dots and effects on biological systems.* Nature Materials, 2006. **5**(5): p. 409-17.

41. Kirchner C, Liedl T, Kudera S, Pellegrino T, Munoz Javier A, Gaub HE, Stolzle S, Fertig N, Parak WJ. *Cytotoxicity of colloidal CdSe and Cdse/ZnS nanoparticles.* Nano Letters, 2005. **5**(2): p. 331-8.

42. Hoshino A, Fujioka K, Oku T, Suga M, Sasaki YF, Ohta T, Yasuhara M, Suzuki K, Yamamoto K. *Physicochemical properties and cellular toxicity of nanocrystal quantum dots depend on their surface modification.* Nano Letters, 2004. **4**(11): p. 2163-2169.

43. Jaiswal JK, Simon SM. *Potentials and pitfalls of fluorescent quantum dots for biological imaging.* Trends in Cell Biology, 2004. **14**(9): p. 497-504.

44. Langer R, Vacanti JP. *Tissue engineering.* Science, 1993. **260**(5110): p. 920-6.

45. Lu Q, Ganesan K, Simionescu DT, Vyavahare NR. *Novel porous aortic elastin and collagen scaffolds for tissue engineering.* Biomaterials, 2004. **25**(22): p. 5227-37.

46. Griffith LG, Naughton G. *Tissue engineering--current challenges and expanding opportunities.* Science, 2002. **295**(5557): p. 1009-14.

47. Ratner BD, Hoffman AS, Schoen FJ, Lemons JE. *Biomaterials science: An introduction to materials in medicine.* MRS Bulletin, 2006. **31**: p. 59.

48. Gao H, Wang YN, Fan YG, Ma JB. *Synthesis of a biodegradable tadpole-shaped polymer via the coupling reaction of polylactide onto mono(6-(2-aminoethyl)amino-6-deoxy)-beta-cyclodextrin and its properties as the new carrier of protein delivery system.* Journal of Control Release, 2005. **107**(1): p. 158-73.

49. Williams ATR, Winfield SA, Miller JN. *Relative fluorescence quantum yields using a computer-controlled luminescence spectrometer.* Analyst, 1983. **108**(1290): p. 1067-1071.

50. Wang Y, Ameer GA, Sheppard BJ, Langer R. *A tough biodegradable elastomer.* Nature Biotechnology, 2002. **20**(6): p. 602-6.

51. Sperling LH. *Introduction to physical polymer science*. 1992: Wiley.

52. Rydholm AE, Held NL, Benoit DS, Bowman CN, Anseth KS. *Modifying network chemistry in thiol-acrylate photopolymers through postpolymerization functionalization to control cell-material interactions.* Journal of Biomedical Materials Research Part A, 2008. **86**(1): p. 23-30.

53. Tsuboi Y, Ikejiri T, Shiga S, Yamada K, Itaya A. *Light can transform the secondary structure of silk protein.* Applied Physics A: Materials Science & Processing, 2001. **73**(5): p. 637-640.

54. Yang J, Webb AR, Pickerill SJ, Hageman G, Ameer GA. *Synthesis and evaluation of poly(diol citrate) biodegradable elastomers.* Biomaterials, 2006. **27**(9): p. 1889-98.

55. Yang J, Webb AR, Ameer GA. *Novel citric acid-based biodegradable elastomers for tissue engineering.* Advanced Materials, 2004. **16**(6): p. 511-516.

56. Kricheldorf HR, Fehrle M. *New polymer syntheses.* Polymer Bulletin, 1981. **6**: p. 21-27.

57. Gachkovskii VF. *Universal fluorescence of polymers.* Zhurnal Strukturnol Khimii, 1967. **8**(2): p. 362-364.

58. Hof M, Hutterer R, Fidler V. *Fluorescence spectroscopy in biology: Advanced methods and their applications to membranes, proteins, DNA, and cells*. 2005: Springer.

59. Song X, Perlstein J, Whitten DG. *Photoreactive supramolecular assemblies: Aggregation and photoisomerization of azobenzene phospholipids in aqueous bilayers.* Journal of the American Chemical Society, 1995. **117**(29): p. 7816-7817.

60. Jenekhe SA, Osaheni JA. *Excimers and exciplexes of conjugated polymers.* Science, 1994. **265**(5173): p. 765-768.

61. Quan S, Teng F, Xu Z, Qian L, Hou Y, Wang Y, Xu X. *Solvent and concentration effects on fluorescence emission in MEH-PPV solution.* European Polymer Journal, 2006. **42**(1): p. 228-233.

62. Rohwer LS, Martin JE. *Measuring the absolute quantum efficiency of luminescent materials.* Journal of Luminescence, 2005. **115**(3-4): p. 77-90.

63. Inouye S. *Blue fluorescent protein from the calcium-sensitive photoprotein aequorin is a heat resistant enzyme, catalyzing the oxidation of coelenterazine.* FEBS Letters, 2004. **577**(1-2): p. 105-10.

64. Patterson G, Day RN, Piston D. *Fluorescent protein spectra.* Journal of Cell Science, 2001. **114**(Pt 5): p. 837-8.

65. Ellenberg J, Lippincott-Schwartz J, Presley JF. *Dual-colour imaging with GFP variants.* Trends in Cell Biology, 1999. **9**(2): p. 52-6.

66. Pepperkok R, Squire A, Geley S, Bastiaens PI. *Simultaneous detection of multiple green fluorescent proteins in live cells by fluorescence lifetime imaging microscopy.* Current Biology, 1999. **9**(5): p. 269-72.

67. Volkmer A, Subramaniam V, Birch DJ, Jovin TM. *One- and two-photon excited fluorescence lifetimes and anisotropy decays of green fluorescent proteins.* Biophysical Journal, 2000. **78**(3): p. 1589-98.

68. Hanley QS, Subramaniam V, Arndt-Jovin DJ, Jovin TM. *Fluorescence lifetime imaging: Multi-point calibration, minimum resolvable differences, and artifact suppression.* Cytometry, 2001. **43**(4): p. 248-60.

69. Cheng FY, Wang SP, Su CH, Tsai TL, Wu PC, Shieh DB, Chen JH, Hsieh PC, Yeh CS. *Stabilizer-free poly(lactide-co-glycolide) nanoparticles for multimodal biomedical probes.* Biomaterials, 2008. **29**(13): p. 2104-12.

70. Feng L, Zhang C, Chen Z, Qin A, Yuan M, Bai F. *Synthesis and characterization of photoluminescent conjugated polymer containing N-(-naphthyl)-carbazole unit.* Journal of Applied Polymer Science, 2006. **100**(2): p. 923.

BIOGRAPHICAL INFORMATION

Santosh Gautam was born in Kavre, Nepal in July of 1982. He finished his high school in his hometown and came to the United States in 2002 for his further education. He attended a junior college from 2002 to 2004 and then joined the University of Texas at Arlington as a biology student in January of 2005. While taking a variety of biology and engineering courses at UTA, he was attracted to the innovative part of Biomedical Engineering. With this understanding, as a dedicated and ambitious personality, he joined the Biomaterials and Tissue Engineering Research Laboratory at UTA in May, 2007. Santosh completed his Bachelor of Science in Biology and Masters of Science in Biomedical Engineering at joint program of University of Texas at Arlington and University of Texas Southwestern Medical Center in August, 2008. He is looking forward to find a job that best fits his academic background, technical skills and work experience in bioengineering field.